Neuropharmacology 158 (2019) 107729

Contents lists available at ScienceDirect

Neuropharmacology

journal homepage: www.elsevier.com/locate/neuropharm

Why flavored vape products may be attractive: Green apple tobacco flavor elicits reward-related behavior, upregulates nAChRs on VTA dopamine neurons, and alters midbrain dopamine and GABA neuron function

Alicia J. Avelar, Austin T. Akers, Zachary J. Baumgard, Skylar Y. Cooper, Gabriella P. Casinelli, Brandon J. Henderson*

Department of Biomedical Sciences, Marshall University, Joan C Edwards School of Medicine, Huntington, WV, USA

HIGHLIGHTS

- Green apple flavorant, farnesol, causes reward-related behavior in male mice.
- Farnesol upregulates α6-containing nAChRs and not α4(non-α6)-containing nAChRs.
- Farnesol enhances the firing frequency of VTA dopamine neurons in male mice.

ARTICLE INFO

Keywords:
Addiction
Vaping
Tobacco
Flavorants
Nicotinic receptors
Dopamine neuron
GABA neuron
Conditioned place preference
Electrophysiology
Microscopy

ABSTRACT

While nicotine is the primary addictive component in tobacco products, additional flavors have become a concern with the growing popularity of electronic nicotine delivery systems (ENDS). For this reason, we have begun to investigate popular tobacco and ENDS flavors. Here, we examined farnesol, a chemical flavorant used in green apple and fruit flavors in ENDS e-liquids, for its ability to produce reward-related behavior. Using male and female 3–6 month old C57BL/6 J mice and farnesol doses of 0.1, 1, and 10 mg/kg we identified a sex-dependent effect in a conditioned place preference assay: farnesol-alone produces reward-related behavior in only male mice. Despite this sex-dependent effect, 1.0 mg/kg farnesol enhances locomotor activity in both male and female mice. To understand farnesol's effect on reward-related behavior, we used whole-cell patch-clamp electrophysiology and confocal microscopy to investigate changes in putative dopamine and GABA neurons. For these approaches, we utilized genetically modified mice that contain fluorescent nicotinic acetylcholine receptors (nAChRs). Our electrophysiological assays with male mice revealed that farnesol treatment increases ventral tegmental area (VTA) dopamine neuron firing frequency and this may be due to a decrease in inhibitory tone from GABA neurons. Our microscopy assays revealed that farnesol treatment produces a significant upregulation of α6* nAChRs in male mice but not female mice. This was supported by an observed increase in α6* nAChR function in additional electrophysiology assays. These data provide evidence that popular tobacco flavorants may alter smoking-related behavior and promote the need to examine additional ENDS flavors.

1. Introduction[1]

Nicotine, the primary addictive component of tobacco and ENDS products, stimulates dopamine neurotransmission through the activation of nAChRs. The key nAChR subtypes that mediate nicotine addiction are most likely α4β2*, α6β2β3, and α4α6β2* nAChRs due to their location on midbrain neurons of the dopamine reward pathway and their high-sensitivity to nicotine (Pons et al., 2008; Kuryatov and Lindstrom, 2011; Liu et al., 2012; Engle et al., 2013). The most popular tobacco flavor, menthol, has been reported to enhance nicotine reward and reinforcement (Wang et al., 2014; Biswas et al., 2016; Henderson et al., 2017) by altering nAChR upregulation (Brody et al., 2013;

* Corresponding author. Department of Biomedical Sciences, Joan C Edwards School of Medicine at Marshall University, 1700 3rd Ave, 410 BBSC, Huntington, WV, 25703, USA.
E-mail address: Hendersonbr@marshall.edu (B.J. Henderson).

[1] Non-standard abbreviations: electronic nicotine delivery systems, ENDS; nAChR, nicotinic acetylcholine receptor; NFRET, normalized Förster resonance energy transfer; SNr, substantia nigra pars reticulata; SNc, substantia nigra pars compacta; VTA, ventral tegmental area.

https://doi.org/10.1016/j.neuropharm.2019.107729
Received 30 March 2019; Received in revised form 22 July 2019; Accepted 28 July 2019
Available online 29 July 2019
0028-3908/

Alsharari et al., 2015; Henderson et al., 2016, 2017), increasing dopamine neuron excitability (Henderson et al., 2017), facilitating nicotine-evoked dopamine release (Zhang et al., 2018), and by acting on transient receptor potential cation channel subfamily melastatin member 8 (TRPM8) to elicit cooling sensations (Wang et al., 2014; Fan et al., 2016) to potentially allow new smokers to overcome the harsh irritation of tobacco inhalation (Dessirier et al., 2001). Ultimately, the greatest concern regarding menthol is the fact that smokers of menthol cigarettes exhibit lower cessation rates compared to non-menthol smokers (Gandhi et al., 2009; Benowitz and Samet, 2011; Hoffman and Miceli, 2011; D'Silva et al., 2012; FDA, 2012).

Given the effect menthol has on nicotine reward, reinforcement, and smoking cessation, it is critical that we understand how other flavors influence smoking behavior. Growing concerns of flavors' effect on ENDS use have caused the FDA to take actions to reduce youth smoking initiation. At the time of this study, the FDA is proposing a ban on menthol flavoring in combustible cigarettes and a measure to restrict sales of flavored ENDS in convenience stores. Given the rapid growth in ENDS popularity among youth, their propensity to choose flavored e-liquids, and the knowledge that flavored tobacco increases smoking initiation among youth, there is a clear need to increase our understanding of tobacco flavors' effects on neurobiology. This is especially true given that ENDS popularity is owed to their flavors (Mead et al., 2019). Despite the attention to youth ENDS use, 70% of adult ENDS users also prefer flavored e-liquids (Schneller et al., 2018). Thus, this is a problem that spans all age ranges.

Many flavorants used in tobacco products exhibit similar chemical scaffolds to menthol. Therefore, we hypothesized that these flavorants may also alter midbrain dopamine neurons in a manner that contributes to reward-related behavior. Among users of ENDS and hookah, green apple flavors are as popular as menthol. According to some reports, green apple and other fruity flavors are more popular than menthol (Omaiye et al., 2019). Thus, we believe that green apple flavorants are a suitable starting point for investigating the effect that ENDS flavors exert on neurobiology. Farnesol is one of the most prominent chemical flavorants and odorants used in apple flavor and aroma (Espino-Diaz et al., 2016). Most notably, farnesol is the most prominent 'natural' biosynthesized flavorant of apples, along with farnesene (Espino-Diaz et al., 2016) and is present in green apple flavored ENDS e-liquids (Aszyk et al., 2018) along with other chemical flavorants (Tierney et al., 2016). Given the structural similarity to menthol, we chose to investigate farnesol first.

To investigate farnesol's effect on reward-related behavior and neurobiology, we designed experiments utilizing: 1) conditioned place preference assays to examine farnesol's effect on reward; 2) whole-cell patch-clamp electrophysiology with mouse brain slices and cultured cells to examine farnesol's effect on putative dopamine and GABA neurons; and 3) confocal microscopy with mice containing fluorescently labeled nAChRs to assess farnesol's effect on nAChR upregulation. In all assays, we use identical drug exposure conditions to ensure our individual assays supported each other. In the case of microscopy assays, the brains we imaged came from the same mice used in our CPP assays. In doing so, we were able to ensure the drug exposure paradigm is matched between behavior and microscopy assays. Using these approaches, we document that farnesol-alone produces reward-related behavior; thereby partly explaining why flavors such as green apple may be popular among ENDs users.

2. Material and methods

2.1. Reagents and dose selection

Nicotine hydrogen tartrate (product number – 1463304) was obtained from Sigma-Aldrich and Farnesol (product number – 119121000) from Acros Organics. Dihydro-β-erythroidine (DhβE) hydrobromide, a β2* nAChR antagonist, was obtained from Tocris (product number – 2349). For all doses reported in assays, concentrations of nicotine, farnesol, and DhβE are given as free base.

Similar to previous investigations into menthol (Henderson et al., 2016, 2017), we estimated the pharmacologically relevant dose of farnesol in regard to nicotine doses in mouse behavior assays. Concentrations of flavor chemicals in e-liquids range from < 1 mg/mL to 362 mg/mL (Tierney et al., 2016; Omaiye et al., 2019) while typical e-liquid concentrations of flavors are ~12 mg/mL (Omaiye et al., 2019). Omaiye et al., reported that > 56% of flavored e-liquids analyzed had a flavorant/nicotine ratio of ≥2. In combustible cigarettes, tobacco flavorants are found to be 2-fold in most cases (flavorant/nicotine ratio) but vary in a range of 1–20 fold (prior to 2009 ban of non-menthol flavors) (Tierney et al., 2016). Nicotine at a dose of 0.5 mg/kg is rewarding in mouse conditioned place preference assays (Tapper et al., 2004; Henderson et al., 2016, 2017). Following this prior evidence that a 2-fold flavorant/nicotine ratio is representative of the cigarette/e-cigarette market, 1.0 mg/kg farnesol is a perceived smoking-relevant and ENDS-relevant dose. To gain additional understanding we added farnesol doses that are one log unit above and below 1.0 mg/kg (0.1–10 mg/kg farnesol) to obtain a limited dose-response relationship. Furthermore, the potency of farnesol in its ability to inhibit nAChRs is similar to menthol (see Fig. 4). Thus, this provides some evidence that the relevant dosing range of farnesol is similar to the 0.1–10 mg/kg doses of menthol we have examined previously (Henderson et al., 2016, 2017). All doses of farnesol and nicotine given for behavioral assays are listed as doses calculated as a free base. For drug applications in electrophysiology assays we list doses that are calculated as a molar concentration.

2.2. Mice

All experiments were conducted in accordance with the guidelines for care and use of animals provided by the National Institutes of Health. Protocols were approved by the Institutional Animal Care and Use Committee at Marshall University. Mice were kept on a standard 12/12 h light/dark cycle at 22 °C and given food and water *ad libitum*. For our assays, we utilized α4-mCherryα6-GFP mice that originated from a C57BL/6 J background (For details regarding α4-mCherryα6-GFP mice see (Henderson et al., 2017). Of the mice used in conditioned place preference assays, the brains of mice that were α4-mCherry/α6-GFP homozygous/transgenic were used in confocal microscopy assays (36 mice, see Fig. 8). The remaining mice used in conditioned place preference assays were the non-transgenic littermates. Thus, all mice used in CPP assays, microscopy, and electrophysiology are from the same strain. The *n* value of male and female mice used in CPP assays are given in detail in Fig. 2.

α4-mCherryα6-GFP mice were produced by crossing α6-GFP BAC transgenic mice (Mackey et al., 2012) to α4-mCherry homozygous knock-in mice (Srinivasan et al., 2016). α6-GFP mice are continuously backcrossed to C57BL/6 J mice (The Jackson Laboratory) while α4-mCherry knock-in mice are backcrossed to C57BL/6 J mice (also, The Jackson Laboratory) every 10 generations. For all behavioral and electrophysiology assays, WT mice were tested in addition to α4-mCherryα6-GFP mice. These included littermate controls and separate C57BL/6 J mice.

2.3. Genotyping

On postnatal day 21, mice were weaned and housed with same-sex littermates, as stipulated by Marshall's University's animal research facility guidelines. Tail biopsies were taken between postnatal day 16–21 for genotyping analysis by PCR. Tails were genotyped using previously published methods (Henderson et al., 2017) by Transnetyx (Cordova, TN). Only mice that were transgenic for α6-GFP and homozygous for α4-mCherry were used in confocal assays (see below), with the exception of α6-GFP-only and α4-mCherry-only mice used for

NFRET controls (see section **2.8**). For all experiments, we used adult (3–6 months old) mice. Both male and female mice were used and numbers of each is given in detail in their corresponding figures.

2.4. Conditioned place preference (CPP) assays

CPP assays were completed with a three-chamber spatial place-preference chamber (Harvard Apparatus, PanLab, dimensions: 47.5 × 27.5 × 47.5 cm) using male and female α4-mCherryα6-GFP mice. Time in chambers was recorded by motion tracking software (SMART 3.0). A 6 day, unbiased protocol identical to previous studies (Henderson et al., 2016, 2017) was used where 'drugs' were given in the white/grey chamber and saline was given in a white/black chamber (intraperitoneal injection). On day 1, mice were placed in the central chamber and allowed free access for 20 min. Mice that spent > 65% of the test in one chamber were excluded and the remaining mice were counterbalanced. For counterbalancing, mice were separated into groups of approximately equal bias, similar to previous published CPP methods (Sanjakdar et al., 2015). Following exclusions (2 male mice, 1 female mouse) and counterbalancing, no initial biases were noted (see Supplemental Fig. 2 for mean data of initial bias for each treatment group). On days 2–4, mice were conditioned using twice-daily sessions where saline injections were given in the black chamber and drugs (farnesol, nicotine, dissolved in pH 7.4 saline) were injected in the white chambers. The duration between drug injections and conditioning was < 1 min as mice were injected and placed directly in the conditioning chamber for their 20 min training period. Between AM and PM conditioning sessions, mice had a ~4 h break. On day 6, mice were given free access to the chamber for 20 min and time spent in all chambers was recorded.

We used the β2* nAChR antagonist, DhβE, to determine if farnesol-induced conditioned place preference may be mediated through nAChRs. For these assays, we pre-injected mice with saline or 2 mg/kg DhβE 15 min prior to an injection of saline or 1.0 mg/kg farnesol. All other parameters of these CPP assays were identical to those described above.

Nearly equal numbers of male and female mice, 3–5 months old, were used in CPP assays (67 males and 75 females total). Sex differences are discussed in *Results*. Locomotor activity (distance traveled) during pre- and post-test recording sessions was not significantly different between the different drug treatment groups (see Fig. 3). Data are expressed as a change in baseline preference between the post- and pre-test:

$$(drug_{paired} - saline_{paired})_{posttest} - (drug_{paired} - saline_{paired})_{pretest}$$

Experimenters were blind to drug treatments until all data analysis for the respective cohort were completed. To blind drug treatments, we had a person, other than the experimenter, make saline and drug solutions and provide a non-descriptive label such as 'solution A'. Once the CPP cohort was complete and mice were scored for the pre-test and post-test, the experimenter was then informed the identity of the blinded solutions. This applied to only the drug-paired days, as the protocol dictates saline is given on saline-paired days. All drugs used in CPP assays were dissolved in saline at pH 7.4 and injected intraperitoneally. We have previously used a 10 day, once-daily CPP protocol to study reward-related behavior and comparisons between our twice-daily and once-daily methods produced similar results (Supplementary Fig. 1).

2.5. Locomotor assays

3–5 month old non-transgenic α4-mCherryα6-GFP mice were habituated to the experimental room for 2 h prior to the experiment. Male or female mice were placed in an open field (40 × 40 × 36 cm) immediately after an intraperitoneal injection of saline or farnesol (1.0 mg/kg). Distance traveled over a period of 20 min was recorded using motion tracking software (SMART 3.0). Number of mice and sex are listed in Fig. 3.

2.6. Whole-cell electrophysiology

Recordings were performed using brain slices prepared from 3 month old male α6-GFP mice. We used α6-GFP mice because α6 nAChR subunits are selectively expressed in dopamine neurons and provide a method to identify putative dopamine neurons. Previous investigations revealed that α6-GFP expression in the VTA and substantia nigra pars compacta (SNc) completely overlaps with the expression of tyrosine hydroxylase (Mackey et al., 2012). To match the investigation of VTA dopamine neurons in microscopy assays, we targeted bregma −3.1 but given the thickness of slices (250 μm), our anterior-posterior limits were bregmas −2.7 to −3.5 mm. Mice were euthanized with CO_2 and were subjected to cardiac perfusion with warm glycerol-based artificial cerebral spinal fluid (GACSF) saturated with 95% O_2/5% CO_2 containing (mM): 250 glycerol, 2.5 KCl, 1.2 NaH_2PO_4, 1.2 $MgCl_2$, 2.4 $CaCl_2$, 26 $NaHCO_3$ and 11 glucose. Coronal sections (250 μm) were cut to contain the VTA and were allowed to recover at 32 °C in carbogenated ACSF, containing (mM): 125 NaCl, 2.5 KCl, 1.2 NaH_2PO_4, 1.2 $MgCl_2$, 2.4 $CaCl_2$, 26 $NaHCO_3$, and 11 glucose for 1 h. For brain slicing, the mouse brain was removed and placed in agarose for slicing with a Compresstome® VF-300-OZ (Precisionary Instruments) while immersed in warm GACSF that was pre-saturated with carbogen. While many tissue slicing methods use ice-cold solutions, the current recommendations for Compresstome slicing suggests cutting with warm solutions (www.precisionary.com). After the 1 h recovery period, slices were transferred to the slice chamber and continually perfused with carbogen-saturated ACSF (1.5–2.0 ml/min) at 32 °C.

Neurons were visualized with an upright microscope (Axio Examiner A1, Zeiss) equipped with an Axiocam 503 mono using DIC near infrared illumination. Blue illumination was used to visualize α6-GFP presence in putative dopamine neurons. Whole-cell patch-clamp techniques were used to record electrophysiological signals with an Integrated Patch-Clamp Amplifier (Sutter). Patch electrodes had resistances of 4–8 MΩ when filled with intrapipette solution (in mM): 135 K gluconate, 5 KCl, 5 EGTA, 0.5 $CaCl_2$, 10 HEPES, 2 Mg-ATP, and 0.1 GTP. Recordings were sampled at 10 KHz. The junction potential between patch pipette and bath solutions was nulled just before gigaseal formation. Series resistance was monitored without compensation throughout experiments using SutterPatch software. The recording sessions for neurons were terminated if the series resistance changed by more than 20%. Nicotine (dissolved in ACSF at pH 7.4) applications were applied using a Picospritzer III (Parker) at 5 psi. Drug concentrations and duration of applications are given in *Results*.

For cultured cells, 50,000 neuro-2a cells were plated onto sterilized 12 mm circular glass coverslips, placed in 35-mm culture dishes and cultured in a humidified incubator (37 °C, 95% air, 5% CO_2). Cells were transfected as described below. For patching of neuro-2a cells we used extracellular solution containing (in mM): 140 NaCl, 5 KCl, 2 $CaCl_2$, 1 $MgCl_2$, 10 HEPES, and 10 glucose (320 mOsm, pH set to 7.3 with Tris-base) similar to previous studies (Henderson et al., 2014, 2016). For voltage-clamp experiments, neuro-2a cells were voltage clamped at a holding potential of −55 mV. To avoid nAChR desensitization by repetitive nicotine application we applied drug puffs at ~3 min intervals and continually perfused the recording chamber with extracellular solution.

2.7. Neuro-2a cell culture and transient transfections

Mouse neuroblastoma 2a (neuro-2a) cells were cultured using standard techniques (Srinivasan et al., 2011). Cells were plated by adding 45,000 cells to poly-12-mm glass coverslips laid in 35 mm dishes and cultured in a humidified incubator (37 °C, 95% air, 5% CO_2). Cells

were transfected with 500 ng of each nAChR subunit cDNA (α4-GFP and β2wt). Plasmids were mixed with 250 μl of Opti-MEM. Lipofectamine-3000 was separately added to 250 μl of Opti-MEM. After 5 min at 24 °C, DNA and lipofectamine solutions were mixed together and incubated for 25 min at 24 °C. The solutions were then added to pre-plated neuro-2a cells and incubated for 24 h. After 24 h, the Opti-MEM was removed and replaced with growth medium. 500 nM filter-sterilized farnesol (or sham treatment) was added after replacing the Opti-MEM with standard culture medium. 24 h after drug/sham addition, neuro-2a cells were used in whole-cell electrophysiology assays. Neuro-2a cells were not allowed to differentiate prior to the assays.

2.8. Confocal imaging of mouse brain slices

No immunofluorescence methods were used in this work. As mentioned above, α4-mCherryα6-GFP mice from CPP assays were used for microscopy assays. Following the completion of CPP assays, mice were euthanized with CO_2 and subjected to a quick cardiac perfusion with 10 mL ice-cold saline. This significantly reduced the autofluorescence in the mCherry emission range (Henderson et al., 2017). The brain was removed and frozen using acetone and dry ice and stored at −80 °C. Brains were coronally sectioned 20 μm thick using a cryostat, mounted with Vectashield (Vector labs, H-1000), and coverslipped. We targeted bregma −3.1 mm because this region gave the most consistent sections that contained a large portion of the VTA, substantia nigra pars reticulata (SNr) and SNc in a single slice. This is also the bregma region we targeted in our brain slice electrophysiology assays. In each session, brain slices were selected according to bregma (anterior-posterior bregmas: 2.9 to −3.3 mm) so that all imaging sessions were matched between animals and across cohorts.

A Leica SP5 TCSII confocal microscope was used to excite α6-GFP and α4-mCherry at 488 and 561 nm, respectively. 20X images with a 10X digital zoom were collected for the quantitative measurements of α4-mCherry and α6-GFP neuron fluorescence intensity. In ImageJ, raw integrated density (RID) was used for the measurements of fluorescence intensity. Normalized Förster resonance energy transfer (NFRET) methods, described previously (Henderson et al., 2017), were used to identify α4α6* nAChRs.

For each mouse, 2 different brain slices were imaged by 2–3 experimenters blind to drug treatment until all data analysis was completed. For each lateral region, 40–60 VTA dopamine neurons and ≥30 VTA GABA neurons were imaged. Data were averaged to provide RID values for each mouse. 36 mice were used in confocal assays, aged 3–5 months (number of mice provided in Fig. 8). Sex differences are discussed in *Results*. Of the CPP mice, 4 males and 4 females were used for each drug treatment and n values for microscopy assays are given in detail in Fig. 8. One α6-GFP mouse brain was imaged with a confocal microscope to make a representative −3.1 bregma coronal montage (see Fig. 5A_2). This was done using identical methods to image α4-mCherryα6-GFP mice.

2.9. Statistical analysis

All results are presented as mean ± SEM and all statistical analyses were performed using Graphpad Prism. Paired data were analyzed by *t*-test (Figs. 3, 6 and 7). To examine potential sex differences, data were analyzed by sex and drug treatment factors using a two-way ANOVA. Where differences were noted, males and females were analyzed separately. CPP and microscopy data were analyzed with a one-way ANOVA or a two-way ANOVA with a *post hoc* Bonferroni for means comparison. We used a power analysis (G*Power software, www.gpower.hhu.de) to determine appropriate sample sizes.

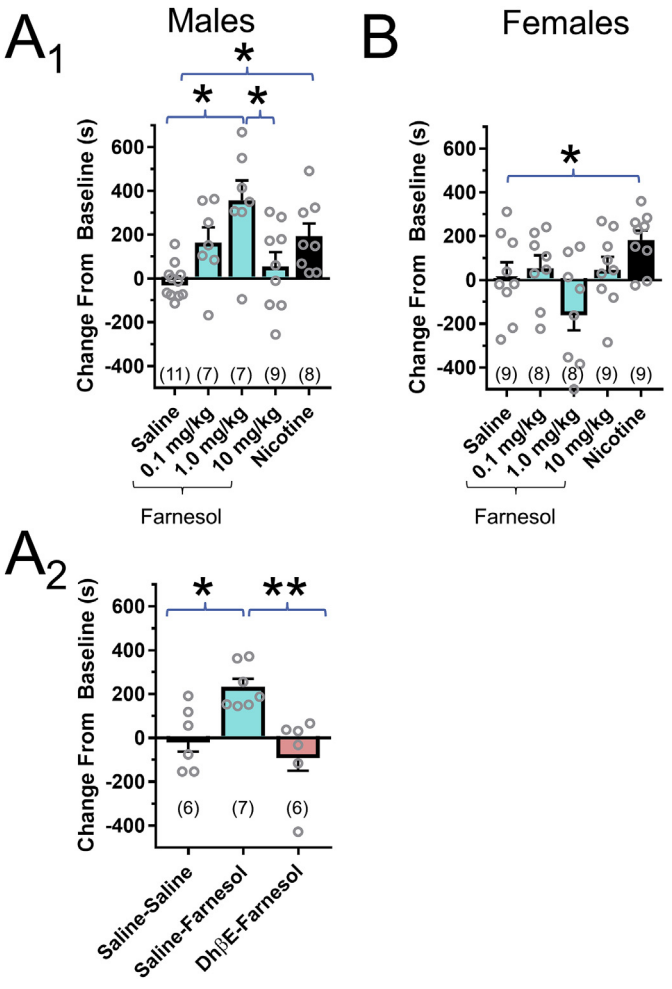

Fig. 1. Farnesol alone produces reward-related behavior in a sex-dependent manner. (A_1 and B) Male and female mice were administered saline, 0.5 mg/kg nicotine, or farnesol at doses 0.1, 1.0, or 10 mg/kg in a CPP assay. (A_2) The β2* nAChR antagonist, DhβE, blocked farnesol-induced CPP in male mice. Mice failed to show significant preference for 1.0 mg/kg farnesol when given a pre-injection of 2 mg/kg DhβE. All data are mean ± SEM. *, $p < 0.05$; **, $p < 0.01$; One-way ANOVA with *post hoc* Bonferroni. Exact *p* values are given in the *Results* section (***3.1***). Number of mice for each treatment group is indicated in parenthesis.

3. Results

3.1. Farnesol alone triggers reward-related behavior in mice

Tobacco flavors have generated concern for public health due to their perceived risk toward increasing smoking initiation (Delnevo et al., 2011; Mead et al., 2019; Schneller et al., 2018). Despite this, few investigations have tested if tobacco flavors (other than menthol) alter reward-related behavior on their own. Based on previous investigations (Henderson et al., 2017), we hypothesized that farnesol would produce no reward-related behavior, by itself, in a CPP assay. To test this hypothesis, we examined farnesol with male and female mice in CPP assays (Fig. 1A and B). For these assays we used α4mCherry-α6GFP mice (Henderson et al., 2017, C57BL/6 J background). Using these mice we planned to conduct follow-up assays where we can directly examine changes in nAChR number as a consequence of changes in reward-related behavior (discussed below, section ***3.6***). We noted sex-dependent effect in our CPP assays with farnesol doses of 0.1, 1, and 10 mg/kg (two-way ANOVA, $F_{(4,\ 77)} = 5.34$, $p = 0.0008$, sex x drug treatment interaction). Therefore we analyzed our CPP data for males and females separately. We observed a significant effect of farnesol treatment with

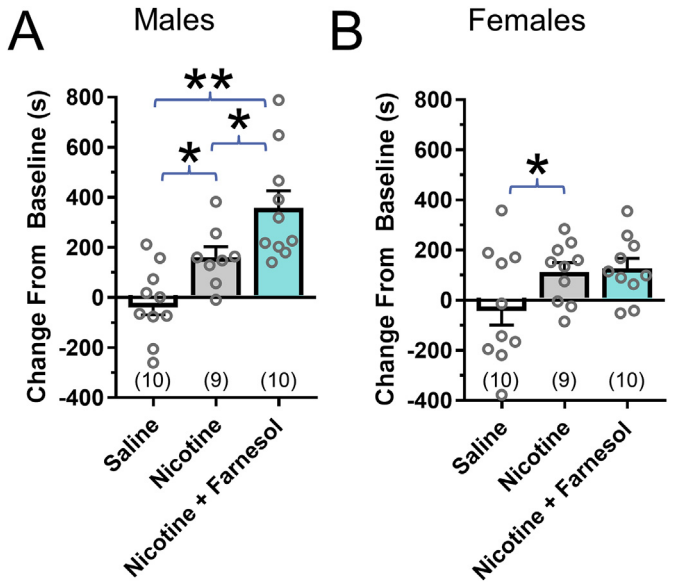

Figure 2. 1.0 mg/kg farnesol increases nicotine conditioned place preference in only male mice. (A and B) Male and female mice were administered saline, nicotine (0.5 mg/kg), or nicotine (0.5 mg/kg) plus farnesol (1.0 mg/kg) in a CPP assay. All data are mean ± SEM. *, $p < 0.05$; **, $p < 0.01$; One-way ANOVA with *post hoc* Bonferroni. Exact *p* values are given in the *Results* section (***3.2***). Number of mice for each treatment group is indicated in parenthesis. Individual dots within bars represent CPP scores from individual mice within the treatment groups.

male mice (one-way ANOVA, $F_{(4,\ 37)} = 5.6$, $p = 0.012$, Fig. 1A$_1$). We observed significant reward-related behavior with 1.0 mg/kg farnesol compared to saline-treated mice ($p = 0.0007$) suggesting that farnesol by itself is rewarding. We also observed a non-significant change from baseline preference with 0.1 mg/kg farnesol in male mice (Fig. 1A$_1$). Similar to the 'inverted U' that is observed in a nicotine dose-response in CPP assays; farnesol produced no reward-related behavior at a dose of 10 mg/kg. We hypothesize that high doses of farnesol (> 10 mg/kg) may be non-rewarding or slightly aversive, similar to high doses of nicotine.

To compare the magnitude of reward-related behavior between farnesol and nicotine, we also used nicotine in our CPP assay (Fig. 1A$_1$ and 1B). We have previously established that an intraperitoneal dose of 0.5 mg/kg nicotine is rewarding in C57BL/6 J and α4-mCherryα6-GFP mice (Henderson et al., 2016, 2017). Here, 0.5 mg/kg nicotine produced significant CPP ($p = 0.01$), similar to previous investigations.

Among female mice, we did observe a significant effect of drug treatment (one-way ANOVA, $F_{(4,\ 38)} = 3.6$, $p = 0.019$, Fig. 2B); but only 0.5 mg/kg nicotine produced reward-related behavior that was significantly different when compared to saline ($p = 0.03$). These data suggest a potential sex-dependent effect of farnesol on reward-related behavior. It is possible that male and female mice exhibit different sensitivities to farnesol and a lower or higher dose range in females may produce an effect in a CPP assay.

To determine if farnesol-induced reward in male mice is mediated through nAChRs, we investigated whether the β2* nAChR antagonist DhβE could block farnesol-induced place-preference (Fig. 1A$_2$). 2 mg/kg DhβE was administered (i.p.) 15 min before a 1.0 mg/kg farnesol injection on conditioning days and resulted in a significant reduction in farnesol place-preference in mice when compared to the cohort of mice that received a saline pre-treatment prior to farnesol injection (one-way ANOVA, $F_{(2,\ 16)} = 8.0$, $p = 0.0039$, Fig. 1A$_2$). These data suggest that the reward-related behavior we observed with farnesol in male mice may be mediated by β2-containing nAChRs.

All of the mice we used in the CPP assays (Fig. 2) failed to exhibit an initial bias for either the saline-paired or drug-paired chambers (Supplemental Fig. 2A$_1$-C$_1$). We also note that there was no change in the distance traveled for each mouse cohort during the CPP pre-test or post-test (Supplemental Fig. 2A$_2$-C$_2$).

3.2. Farnesol increases nicotine reward-related behavior in male mice

While the focus of this investigation is to determine farnesol's direct effect on reward-related behavior in the absence of nicotine, it is important to determine how farnesol alters nicotine reward-related behavior. For this reason, we used a CPP assay to determine if farnesol could increase nicotine reward-related behavior in mice. Similar to the CPP assays discussed in section ***3.1***, we compared co-treatment of 1.0 mg/kg farnesol and 0.5 mg/kg nicotine to 0.5 mg/kg nicotine alone (Fig. 2). In both male and female mice we noted a significant effect of drug treatments when tested with a one-way ANOVA (males, $F_{(2,\ 26)} = 11.0$, $p = 0.0004$; females, $F_{(2,\ 26)} = 3.8$, $p = 0.037$). Males and females also were observed to exhibit nicotine reward-related behavior ($p = 0.014$ and 0.046 for males and females, respectively, Fig. 2A and B). When comparing nicotine and nicotine plus farnesol treatment groups, we only noted a significant difference in male mice ($p = 0.044$) (Fig. 2A). These data show that farnesol significantly increases nicotine-reward related behavior; but only in male mice. Following the observation that farnesol itself produced reward-related behavior, it is likely that nicotine and farnesol have an additive effect, rather than one enhancing the other. These data suggest that green apple flavors that include farnesol may alter smoking-related behavior for all products including nicotine.

3.3. Acute farnesol increases locomotor activity

Spontaneous changes in locomotor activity are considered an excellent preclinical indicator of exogenous drugs that are active in the CNS (Lynch and Mittelstadt, 2009). Additionally, locomotor responses in rodents are considered an index of animal exploration and anxiety that can provide a predictive factor for responses to rewarding drugs (Antoniou et al., 2008). Nicotine's effect on locomotor activity is well characterized and has been consistently reported to increase mouse locomotor behavior (Cohen et al., 2012; Wall et al., 2017). To gain additional measures of CNS activity we used acute intraperitoneal injections of farnesol (1.0 mg/kg) to examine changes in spontaneous locomotor activity in an open field environment. Male and female mice were injected with saline or farnesol (1.0 mg/kg) and their locomotor activity in a novel open field was recorded (Fig. 3A and B). Farnesol significantly increased the distance traveled in both male ($p = 0.0013$, *t*-test) and female ($p = 0.0036$, *t*-test) mice compared to saline-injected mice (Fig. 3). These locomotor data support the hypothesis that farnesol may be a CNS-active flavorant.

3.4. Farnesol alters inhibits α4β2 nAChR function and desensitization

While there are many chemical flavorants used for green apple flavors in tobacco and ENDS products (Tierney et al., 2016; Aszyk et al., 2018), we chose to start our investigations with farnesol because it is a terpene that shares some structural elements with menthol (Fig. 4A$_{1\text{-}3}$). Menthol was previously shown to inhibit α4β2 nAChR inward currents with an IC_{50} of 111 μM (Hans et al., 2012). We investigated whether farnesol could also inhibit α4β2 nAChRs. To do this, we used whole-cell patch-clamp electrophysiology and methods similar to previous investigations to examine concentration-response relationships on α4β2 nAChRs (Henderson et al., 2014, 2016). Neuroblastoma-2a cells were transiently transfected with mouse α4-GFP and mouse β2 nAChR subunits (Fig. 4B$_{1\text{-}2}$). Previous investigations have shown that fluorescently-labeled nAChRs behave the same as unlabeled subunits in regard to trafficking and function (Nashmi et al., 2003; Drenan et al., 2008; Srinivasan et al., 2011) and do not alter rodent behavior when expressed in mice (Nashmi et al., 2007). We stimulated α4β2 nAChRs

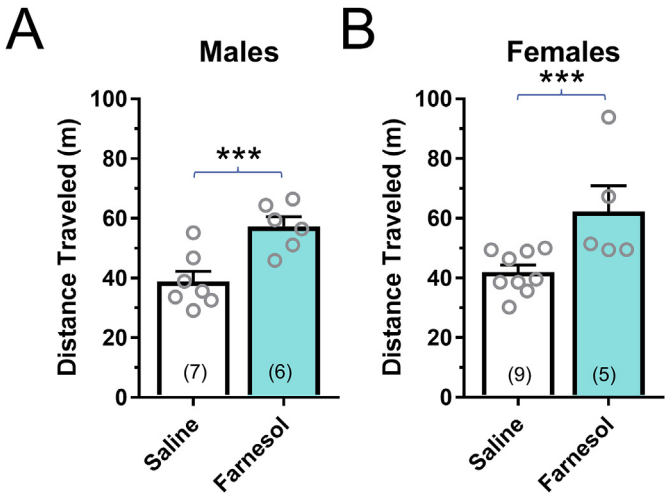

Fig. 3. Acute farnesol treatment increases locomotor activity in an open field. (A–B) Immediately following an intraperitoneal injection of saline or 1.0 mg/kg farnesol, male and female mice were placed in an open field and distance traveled was measured over a duration of 20 min. All data are mean ± SEM. ***, $p < 0.005$; unpaired *t*-test. Exact *p* values are given in the *Results* section (***3.3***). The number of mice from saline- and farnesol-treated cohorts is indicated in parenthesis.

with 10 μM nicotine. While this concentration of nicotine is not smoking-relevant, it stimulates both high-sensitivity and low-sensitivity α4β2 nAChRs robustly and produces maximal nAChR-mediated inward currents in our electrophysiology assays. Here, we observed that farnesol inhibited α4β2 nAChR inward currents with an IC_{50} of 130 ± 9.4 μM (Fig. 4$C_{1\text{-}2}$). We also observed farnesol-induced inhibition of α4β2 nAChRs in a calcium flux assay with a similar IC_{50} value (93.3 ± 21.1 μM, see Supplemental Fig. 3). Thus, we can conclude that farnesol inhibits α4β2 nAChR function; albeit at concentrations that may not be smoking relevant (> 100 μm).

Next, we continued to study how long-term farnesol exposure alters nAChR function using whole-cell patch-clamp electrophysiology. Similar to the previous study of farnesol-induced inhibition, we used neuro-2a cells transiently transfected with α4-GFPβ2 nAChRs (Fig. 4D_1) to test how farnesol treatment alters α4β2 nAChR desensitization and recovery. For these *in vitro* long-term exposure assays, we selected a concentration of farnesol based upon the similarities we have observed between farnesol and menthol (similar inhibitory IC_{50} and similar effective dose range, 1.0 mg/kg, in CPP assays). Previously we have observed that 0.5 μM menthol altered the desensitization of both α4β2 and α6β2β3 nAChRs in neuro-2a cells (Henderson et al., 2016). This dose also was sufficient to alter cultured dopamine neuron excitability (Henderson et al., 2017). For this reason, we treated neuro-2a cells transiently transfected with α4-GFPβ2 nAChRs with 0.5 μM farnesol for 24 h (Fig. 4$D_{1\text{-}2}$). To examine desensitization, we established a baseline for inward currents by stimulating with 10 μM nicotine using 300 ms puff applications repeated at 3 min intervals. Similar to our studies

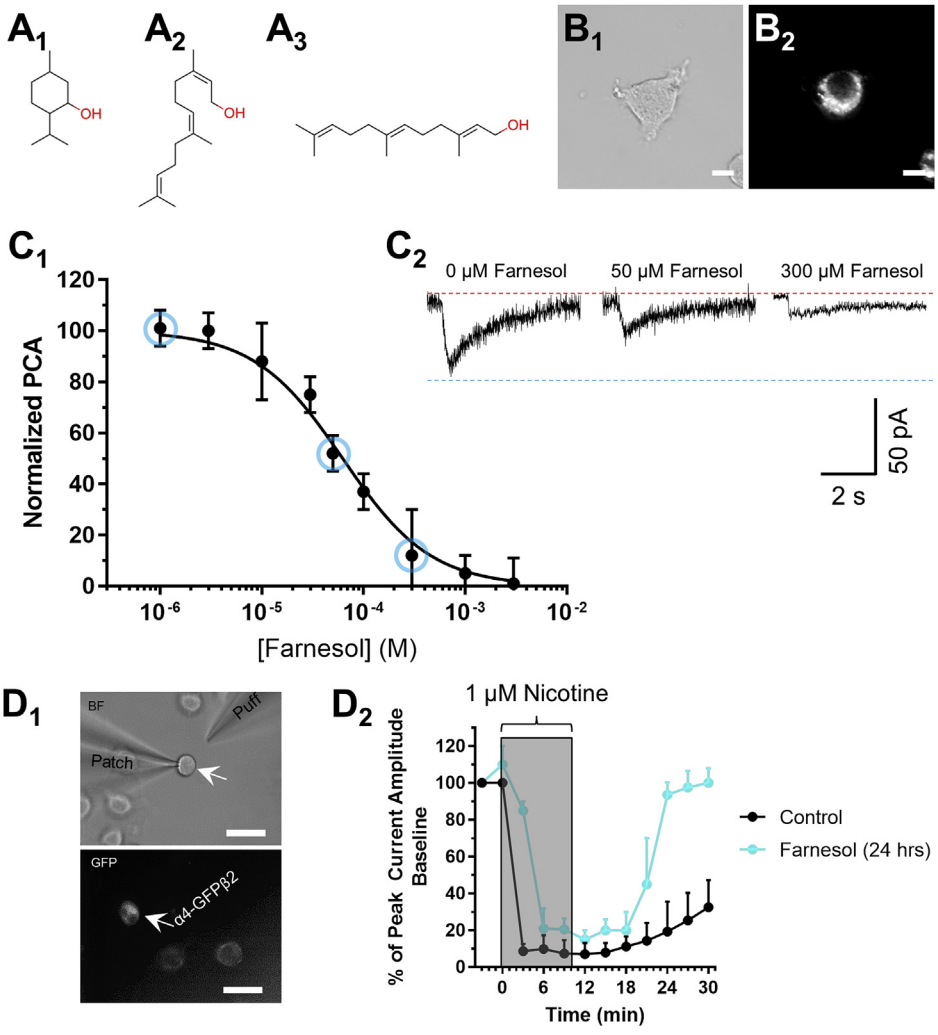

Fig. 4. Farnesol inhibits α4β2 nAChR function. Chemical structure of menthol ($A_{1\text{-}3}$) and farnesol: arranged to exhibit its similarity to menthol (A_2) and its chain orientation (A_3). ($B_{1\text{-}2}$) Neuro-2a cells transiently transfected with α4-GFPβ2 nAChRs in brightfield (B_1) and GFP (B_2) imaging modes. ($C_{1\text{-}2}$) α4-GFPβ2 nAChRs were stimulated with 10 μM nicotine while exposed to increasing concentrations of farnesol to examine its concentration-response on nicotine-stimulated inward currents. (C_1) Mean peak current amplitude (PCA) normalized to 10 μM nicotine. Each data point represents the mean ± SEM of 5–7 neuro-2a cells. (C_2) Representative nicotine-stimulated (10 μM, 300 ms puff) inward currents recorded from neuro-2a cells transiently transfected with α4-GFPβ2 nAChRs exposed to 0, 50, and 300 μM farnesol. Blue circles in C_1 correspond to the representative waveforms in C_2. (D_1) Representative brightfield and GFP images of neuro-2a cells transfected with α4-GFP and β2 nAChR subunits (scale bar, 25 μm). (D_2) Normalized peak current amplitudes of α4-GFPβ2 nAChRs transiently transfected in neuro-2a cells. Cells were treated with no drug (control, black) or farnesol (blue, 0.5 μM for 24 h). nAChRs were desensitized with a 10 min 1 μM nicotine bath perfusion and then allowed to recover for 20 min. Before, during, and after this process, 10 μM nicotine was applied (300 ms puff at 3-min intervals) to stimulate nAChR inward currents (n = 4–5 cells for each data point). (For interpretation of the references to colour in this figure legend, the reader is referred to the Web version of this article.)

focused on inhibition, we selected this concentration because it provides maximal peak current amplitudes with α4β2 nAChRs. Also, the 3 min intervals are sufficient in length to allow nAChRs to recover and not contribute to desensitization (Xiao et al., 2011, 2015; Henderson et al., 2016). Following test pulses, we then bath perfused 1 μM nicotine for 10 min to ensure desensitization of α4β2 nAChRs. Several previous reports have indicated that bath perfusion of 1 μM nicotine is sufficient to completely desensitize β2-containing nAChRs (Xiao et al., 2011, 2015; Henderson et al., 2016). We continued to puff 10 μM nicotine at 3 min intervals to observe the desensitization of the α4-GFPβ2 nAChRs (Fig. 4D_2). At the end of the 10 min, the bath perfusion of 1 μM nicotine stopped and we continued to puff 10 μM nicotine to observe the recovery of α4-GFPβ2 nAChRs (Fig. 4D_2). Flow rates of the solutions were kept constant to ensure there were no differences in washout rates. For untreated α4-GFPβ2 nAChRs, we observed that 1 μM nicotine desensitized inward currents to ~10% of baseline peak current amplitude. After 20 min of recovery, the untreated α4-GFPβ2 nAChRs recovered up to 35% of baseline function. Following 24 h of 0.5 μM farnesol treatment, we observed that α4-GFPβ2 nAChR desensitized to ~20% of baseline peak current amplitude but fully recovered ~17 min after ending the 1 μM nicotine bath perfusion. These data suggest that long-term farnesol treatment may facilitate α4β2 nAChR recovery, following desensitization.

3.5. Farnesol alters putative dopamine and GABA neuron function in mouse brain slices

Many nAChR ligands alter the function of nAChRs on VTA dopamine neurons which then alters dopamine neuron function (Henderson and Lester, 2015). To examine how farnesol alters VTA dopamine neurons, we utilized whole-cell patch-clamp electrophysiology with male and female mouse brain slices (bregma −3.1, Fig. 5A_1). To aid in the identification of dopamine neurons we used α6-GFP mice (Fig. 5$A_{2\text{-}3}$)(Henderson et al., 2016, 2017). α6 nAChR subunits are selectively expressed in dopamine neurons (in the VTA) and they show almost complete overlap with the presence of tyrosine hydroxylase (> 97% of α6-GFP neurons are TH-expressing putative dopamine neurons) (Mackey et al., 2012). α6 nAChR subunits are not present in non-dopamine neurons in the VTA and SNc and are absent in the SNr (Fig. 5A_2). Therefore, α6-GFP presence is an excellent marker for dopamine neurons in the VTA and SNc. Each GFP-positive neuron was also assessed for I_h and action potential durations (> 2 ms). Those containing α6-GFP, I_h, and > 2 ms spike durations were categorized as putative dopamine (pDA) neurons. Coronal brain slices containing the VTA were prepared from α6-GFP mice treated with saline or 1.0 mg/kg farnesol using daily injections that matched our CPP dosing paradigm exactly. We targeted VTA dopamine neurons at bregma −3.1 to match our microscopy assays (see section *3.6* for microscopy assays).

In male and female mice, we detected a sex-dependent effect on farnesol's ability to alter pDA neuron baseline firing frequency (two-way ANOVA, $F_{(1,\ 29)} = 11.6$, $p = 0.002$, sex x drug treatment interaction). For this reason, we analyzed our data separately for male and female mice (Fig. 5). In male mice, we examined baseline firing of pDA neurons and noted a ~5-fold increase in firing frequency when farnesol-treated pDA neurons (11.1 ± 2.4 Hz) were compared to saline-treated neurons (2.1 ± 0.6 Hz) (Fig. 5$B_{1,\ 3}$). In female mice we did not detect a change in pDA firing frequency (Fig. 5$B_{2\text{-}3}$). This result helps explain why female mice were not observed to exhibit reward-related behavior with this dose of farnesol. Given that changes in I_h can alter the tonic firing of dopamine neurons (Deng et al., 2007), we investigated how farnesol treatment alters I_h density (Fig. 5$C_{1\text{-}2}$). Using a series of hyperpolarizing steps, we studied the current-voltage relationship of pDA neurons recorded from male mice treated with saline or farnesol. Although we note a slight decrease in I_h amplitude from farnesol-treated mice, we observed no significant difference in I_h between saline and farnesol treatment groups (two-way ANOVA, drug treatment, $F_{(1,\ 56)} = 2.47$, $p = 0.12$). Thus, farnesol-induced changes in VTA pDA neuron firing frequency cannot be attributed to changes in I_h.

Another way that VTA dopamine neuron firing can be altered is through changes in inhibitory tone from GABA neurons. Previous investigations into long-term nicotine treatment have determined that changes in midbrain DA neuron firing is caused by changes in midbrain GABA neurons (Mansvelder et al., 2002; Nashmi et al., 2007; Xiao et al., 2009). For this reason we investigated how farnesol treatment altered baseline firing of GABA neurons.

We targeted putative GABA (pGABA) neurons in the substantia nigra pars reticulata (SNr) to provide symmetry with previous investigations into nicotine-related reward mechanisms (Nashmi et al., 2007; Xiao et al., 2009). Here we observed pGABA neurons from saline-treated male mice exhibited a firing frequency of 12.8 ± 1.6 Hz while pGABA neurons from farnesol-treated mice exhibited a significant decrease to 8.74 ± 1.1 Hz ($p = 0.047$) (Fig. 6$B_{1\text{-}3}$). This suggests that the increase in pDA neuron baseline firing frequency may be due to a decrease in inhibitory tone from GABA neurons.

Next, we examined how the firing frequency of these pDA neurons were altered when acutely exposed to smoking-relevant concentrations of nicotine. To do this, we applied 500 nM nicotine (peak nicotine concentration following a puff on a cigarette or ENDS) for a duration of 10 s. During nicotine applications, pDA neurons from saline-treated male mice exhibited an increase in firing frequency from 2.7 ± 0.4 Hz to 5.2 ± 1.6 Hz (Fig. 7A_1 and 7B_1, not significant, $p = 0.15$) similar to previous studies (Liu et al., 2012). Despite exhibiting elevated firing frequencies at baseline conditions, pDA neurons from farnesol-treated mice also exhibited a ~2-fold increase in firing frequency ($p = 0.012$, Fig. 7A_2, 7B_2). Thus, farnesol-treated pDA neurons exhibit the same fold-increase in excitability as saline-treated neurons but exhibit a 4-fold increase in maximum firing frequency when compared to pDA neurons in saline-treated male mice. We used similar methods to examine nicotine-induced changes in VTA pDA neuron firing frequency, with and without farnesol treatment, in female mice (Supplemental Fig. 4). In both saline and farnesol-treated female mice we noted a significant increase in pDA neuron firing frequency during acute 500 nM nicotine applications ($p = 0.045$ and 0.021, respective, Supplemental Fig. 4). Despite this, we noted no difference between saline and farnesol-treated female mice in pre- or post-puff firing frequency (two-way ANOVA, $F_{(1,\ 16)} < 0.1$, $p = 0.99$).

Similar to pDA neurons, we stimulated SNr pGABA neurons with nicotine (500 nM, 10 s, Fig. 7$C_{1\text{-}2}$ and 7$D_{1\text{-}3}$). pGABA neurons from saline-treated mice exhibited a ~1.5-fold increase in firing frequency (not significant) (Fig. 7C_1 and 7D_1), similar to what has been observed with stimulation of GABA neurons with 1 μM nicotine (Nashmi et al., 2007). pGABA neurons from farnesol-treated mice exhibited a 2-fold increase in firing frequency ($p = 0.022$) during acute application of nicotine (Fig. 7C_2 and 7D_2). We note that the nicotine-induced elevations in pGABA firing frequency between saline and farnesol treatments did not differ (18.3 ± 2.75 Hz and 19.5 ± 3.52 Hz for saline-treated and farnesol-treated, respectively). This suggests that while farnesol may reduce the baseline firing frequency of GABA neurons, it did not prevent these neurons from reaching the elevated firing frequencies that we observed with 'control' neurons during nicotine stimulation.

Finally, we tested acute applications of farnesol (in male mice) to determine if farnesol can directly alter dopamine or GABA neuron firing. We applied 3 μM farnesol to current-clamped pDA and pGABA neurons and recorded firing frequencies before, during, and after a 10 s puff (Fig. 7B_3 and 7D_3). We chose 3 μM farnesol because this dose is near the threshold for inhibition (Fig. 4C_1). Also, previous investigations suggest that pharmacologically doses of terpene flavorants produce brain concentrations < 2 μM (Henderson et al., 2016). Thus, 3 μM is approximately the upper limit of the perceived pharmacologically-relevant dose. In both pDA and pGABA neurons, acute applications of 3 μM farnesol produced no significant change in firing frequency (Fig. 7B_3 and 7D_3; $p = 0.94$ and 0.76 for pDA and pGABA neurons,

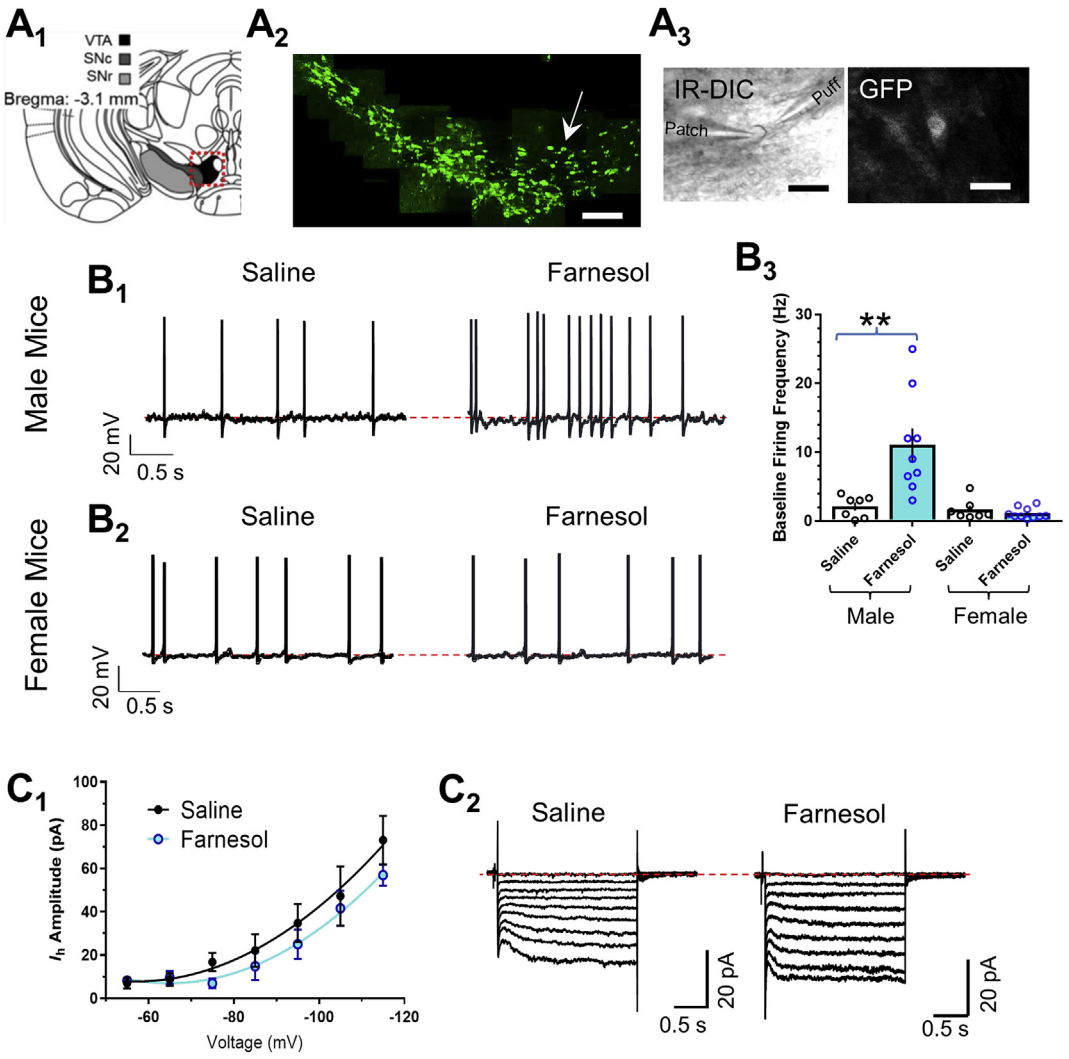

Fig. 5. Farnesol treatment alters function of VTA pDA neurons. For brain slice electrophysiology assays, male and female α6-GFP mice were treated in a manner identical to CPP assays. (A_{1-3}) VTA pDA neurons (target bregma −3.1) were selected by the presence of α6-GFP nAChRs. (A_1) Sample schematic of target VTA at bregma −3.1. (A_2) Sample montage of an α6-GFP mouse brain slice at bregma −3.1. The arrow designates our target VTA pDA neurons were in the lateral as opposed to the medial regions of the VTA. Scale bars: 100 μm (A_2) and 20 μm (A_3). (B_{1-2}) Representative current clamp traces of baseline firing in VTA pDA neurons from saline-treated or farnesol-treated male (B_1) and female (B_2) mice. (B_3) Mean baseline firing frequency (mean ± SEM) for saline-treated (n = 7 neurons total from male 4 mice; 10 neurons from 4 female mice) and farnesol-treated (n = 10 neurons from 4 male mice; 10 neurons from 4 female mice). (C_1) The current-voltage relationship from a series of hyperpolarizing steps to initiate I_h currents in pDA neurons of male mice (n = 4 neurons, 3 mice and 5 neurons, 4 mice for saline and farnesol-treated mice, respectively). (C_2) Representative waveforms from hyperpolarizing voltage step recordings. *, $p < 0.05$; **, $p < 0.01$; unpaired *t*-test. Exact *p* values are given in the *Results* section (***3.5***).

respectively).

3.6. Farnesol upregulates nAChRs in VTA dopamine and GABA neurons

The upregulation of nAChRs following chronic nicotine exposure is a long-studied phenomenon. While upregulation has not been determined to be causal of addictive behavior, it has been determined to be a consequence of long-term nicotine exposure in humans (Mukhin et al., 2008; Brody et al., 2013; Jasinska et al., 2014), rodents (Nashmi et al., 2007; Perez et al., 2008; Henderson et al., 2014), cultured neurons (Srinivasan et al., 2016), and cell lines (Nashmi et al., 2003; Sallette et al., 2005). Many nicotinic ligands upregulate nAChRs (Brody et al., 2013; Henderson et al., 2016, 2017); Therefore, we examined if farnesol treatment upregulated nAChRs on midbrain neurons.

Similar to previous investigations (Henderson et al., 2017), we used α4-mCherryα6-GFP mice from our CPP assays to examine nAChR upregulation after treatment with saline, nicotine, or farnesol. Following CPP assays, coronal mouse brain slices containing the VTA (bregma, −3.1 to match electrophysiology assays) were prepared for microscopy to investigate the upregulation of nAChRs (Fig. 8A_1 and 8A_2). Because these mice came from our CPP cohort, all dosing was administered using daily intraperitoneal injections of drug (saline, 0.5 mg/kg nicotine, 1.0 mg/kg farnesol, or 0.5 mg/kg nicotine plus 1.0 mg/kg farnesol). Using FRET methods, we identified regions of neurons that contain α4α6β2* nAChRs (Henderson et al., 2017) (Fig. 8B). Similar to electrophysiology assays, the presence of α6-GFP was used to distinguish between pDA and pGABA neurons in the VTA (Fig. 8B). Upregulation of nAChRs was assessed by quantifying the change in raw integrated density (RID) of α6-GFP or α4-mCherry fluorescence (Fig. 8C_{1-2} and 8D_{1-2}).

In examining male and female α4-mCherryα6-GFP mice, we noted no difference between sexes when considering upregulation of α4* or α4α6* nAChRs on VTA dopamine neurons or α4* nAChRs on SNr GABA neurons (2-way ANOVA, $F_{(3,\ 28)} = 0.37$, $p = 0.77$ (α4* nAChRs) and $F_{(3,\ 28)} = 0.17$, $p = 0.92$ (α4α6* nAChRs)). We did note a sex-dependent effect with the upregulation of α6* nAChRs on VTA dopamine neurons

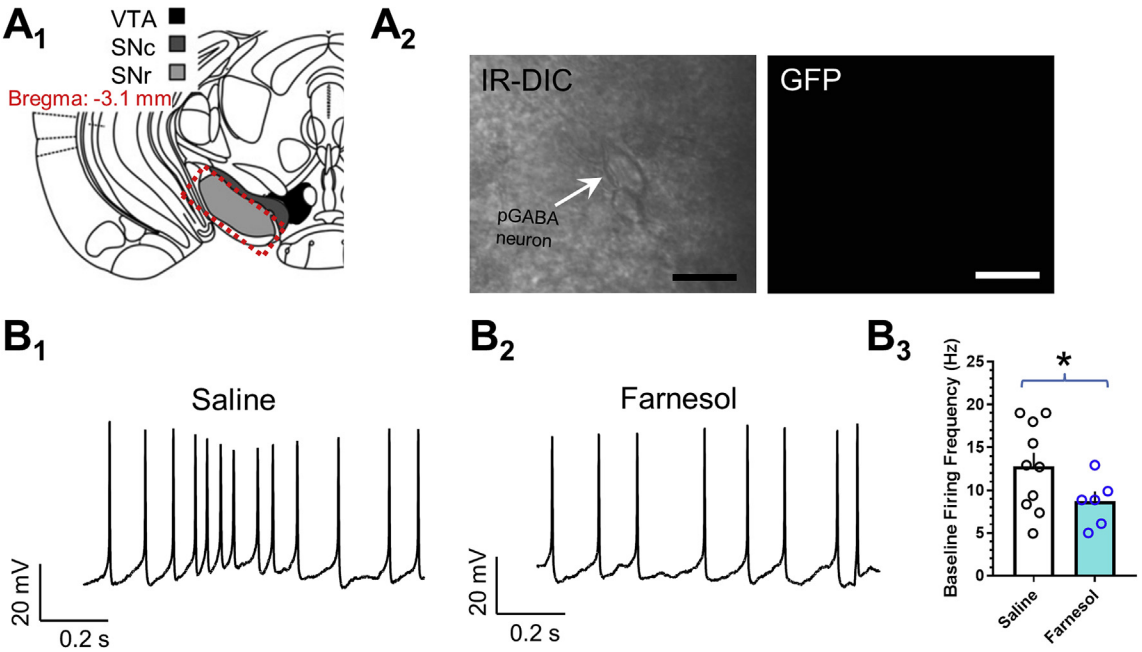

Fig. 6. Farnesol treatment decreases baseline firing frequency of putative SNr GABA neurons in male mice. (A_1) Schematic of target SNr GABA neurons at bregma −3.1. (A_2) Sample images of a SNr pGABA neuron visualized in IR-DIC and fluorescence modes. All pGABA neurons recorded were negative for α6-GFP fluorescence, evidence that they are not dopamine neurons. Scale bars, 20 μm. ($B_{1\text{-}2}$) Representative current clamp recordings from pGABA neurons recorded in brain slices of saline- and 1.0 mg/kg farnesol-treated male mice (treatments identical to CPP dosing paradigm). (B_3) Mean firing frequency of pGABA neurons from saline-treated (n = 10 neurons, 3 mice) and farnesol-treated (n = 6 neurons, 3 mice) male mice. *, $p < 0.05$; unpaired *t*-test. Exact *p* values are given in the *Results* section (***3.5***).

(2-way ANOVA, $F_{(3,\ 28)} = 3.4$, $p = 0.032$, sex x drug treatment interaction). Accordingly, we assessed nAChR upregulation separately for males and females.

In VTA pDA neurons of male mice we noted a significant drug effect on α4*, α6*, and α4α6* nAChR upregulation using a one-way ANOVA ($F_{(2,\ 12)} = 11.4$, $p = 0.0017$; $F_{(2,\ 12)} = 28.5$, $p = 0.0001$; and $F_{(2,\ 12)} = 6.54$, $p = 0.01$ for α4*, α6*, and α4α6* nAChRs, respectively). Male mice treated with nicotine exhibited a significant increase in the RID of α4* ($p = 0.0014$, Fig. 8C_1) and α4α6* ($p = 0.048$, Fig. 8C_1) nAChRs. As we have seen previously (Henderson et al., 2017), we did not observe any change in α6* nAChR RID following treatment with 0.5 mg/kg nicotine (Fig. 8C_1). Male mice treated with 1.0 mg/kg farnesol exhibited a significant increase in the RID of α6* ($p = 0.0001$) and α4α6* ($p = 0.01$) nAChRs but we saw no effect on α4* nAChR upregulation (Fig. 8C_1).

In female mice, we did not observe a significant effect of drug treatment on α6* or α4α6* nAChRs in VTA pDA neurons (Fig. 8D_1; $F_{(2,\ 9)} = 1.19$, $p = 0.35$ and $F_{(2,\ 9)} = 2.46$, $p = 0.14$ for α6* and α4α6*, respectively). We did observe a significant effect of drug treatment in female mice with α4* nAChRs ($F_{(3,\ 14)} = 4.36$, $p = 0.047$, Fig. 8D_1). Here, we observed a significant increase in α4* nAChR RID following nicotine treatment ($p = 0.041$).

In SNr pGABA neurons of male mice, we noted a significant drug effect with α4* nAChRs ($F_{(2,\ 12)} = 30.1$, $p = 0.0001$). Similar to previous observations (Nashmi et al., 2007), nicotine-treated male mice exhibited a significant upregulation of α4* nAChRs on SNr GABA neurons ($p = 0.012$, Fig. 8C_2). With SNr GABA neurons, farnesol-treated male mice exhibited a significant decrease ($p = 0.03$) in α4* nAChR RID (Fig. 8C_2). Since inward currents from nAChRs contributes to depolarizing cells, this decrease in SNr α4* nAChR number may explain why the firing frequency of SNr pGABA neurons decreased with chronic farnesol treatment.

In SNr GABA neurons of female mice, we did not observe a significant effect with drug treatment with female mice (Fig. 8D_2, $F_{(3,\ 12)} = 3.35$ and $p = 0.088$). While many of these trends are similar among male and female mice, there is a clear sex-dependent effect of farnesol on α6* nAChRs. While there is zero effect noted with female mice, we observed a robust increase in α6* nAChR RID in male mice with farnesol treatment. This is likely an important key to understanding why we have observed a sex-dependent effect in our CPP assays using 1.0 mg/kg farnesol.

Similar to our CPP assays using nicotine plus farnesol, we also examined nAChR upregulation following nicotine plus farnesol treatment. Similar to the other treatment groups, these mice came from our CPP assays and were thus exposed to the same dosing regimen. In both male and female mice, nicotine plus farnesol exhibited effects that were similar to nicotine alone in regard to α4* and α4α6* nAChRs (Fig. 8C_1 and 8D_1). Despite the observed additive effect we noted in our CPP assays with male mice, we noted no additive or enhancing effect in regard to nAChR upregulation. We observed that nicotine plus farnesol seemed to counteract the effect of farnesol-alone to upregulate α6* nAChRs on VTA pDA neurons (Fig. 8C_1). Also, nicotine plus farnesol decreased the effect of nicotine-alone on α4* nAChR upregulation on SNr GABA neurons (Fig. 8C_2). These competing effects on nAChR upregulation could be a result of farnesol and nicotine acting as a chaperone for different subtypes of nAChRs as has been documented previously (Henderson and Lester, 2015; Henderson et al., 2016). Some evidence for this exists in the fact that farnesol seems to robustly upregulate α6* nAChRs while nicotine robustly upregulates α4* nAChRs.

3.7. Functional upregulation of α6* nAChRs

While our *in vivo* upregulation assays allow a region and cell-specific examination of nAChR upregulation, this technique does not answer the question of functional upregulation. To determine if farnesol treatment causes functional upregulation of nAChRs, we once again employed whole-cell patch-clamp electrophysiology. Given the complex arrangement of nAChR subtypes in VTA dopamine neurons (α4β2, α4α6β2, α6β2, and more), we decided to transiently transfect specific nAChR subtypes into neuro-2a cells (Fig. 9). We treated neuro-2a cells

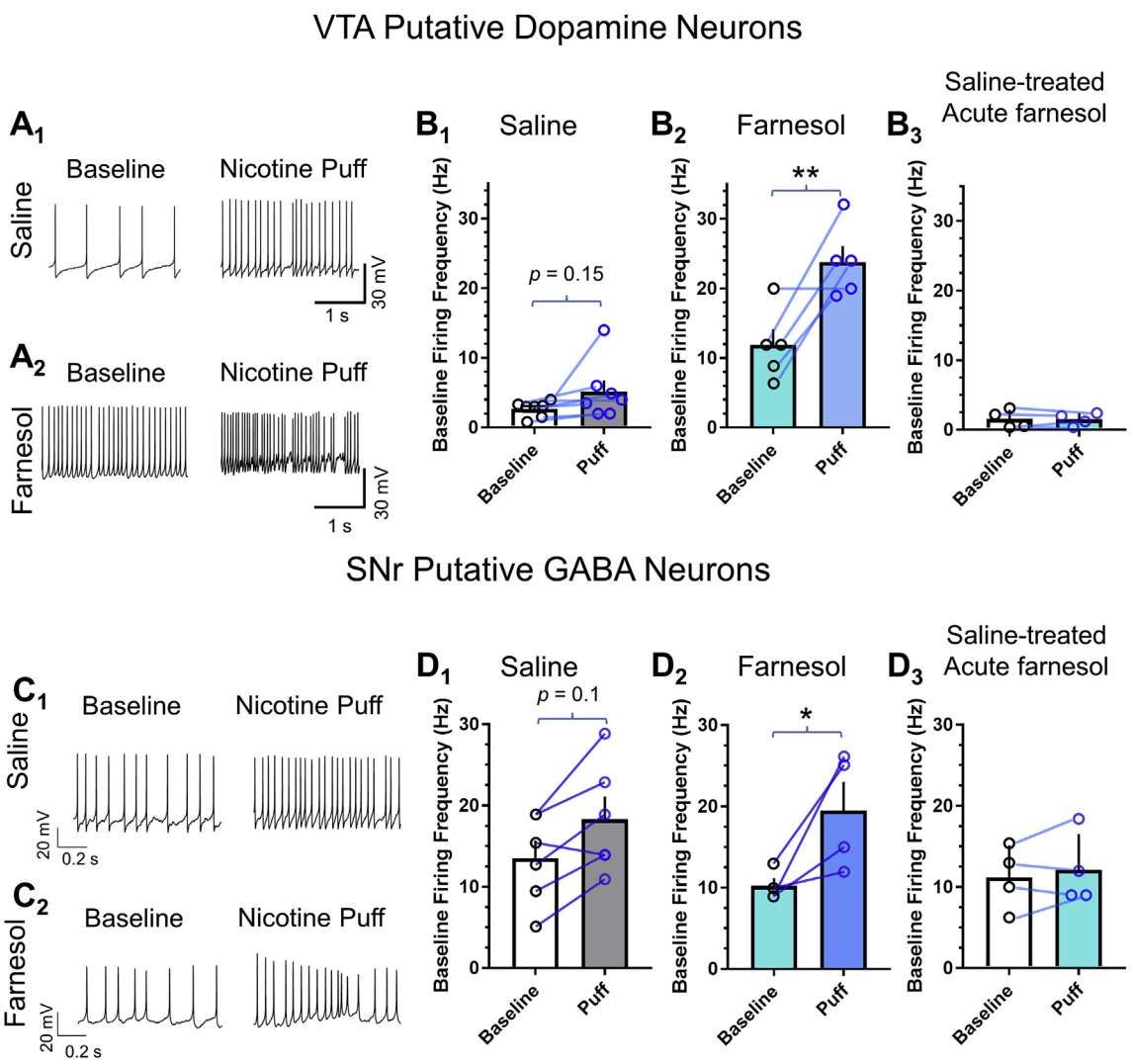

Fig. 7. Acute nicotine exposure increases baseline firing frequency of putative DA and GABA neurons in male mice. ($A_{1\text{-}2}$) Representative current clamp recordings of VTA pDA neurons recorded prior to (left) and during 10 s, 500 nM nicotine application (right). ($B_{1\text{-}2}$) Mean firing frequency before and during nicotine application (mean ± SEM) for saline-treated (n = 6 neurons total from 5 mice) and farnesol-treated pDA neurons (n = 5 neurons from 4 mice). ($C_{1\text{-}2}$) Representative current clamp recordings of SNr pGABA neurons recorded prior to (left) and during 10 s, 500 nM nicotine application (right). ($D_{1\text{-}2}$) Mean firing frequency before and during nicotine application (mean ± SEM) for saline-treated (n = 5 neurons total from 3 mice) and farnesol-treated (n = 4 neurons from 3 mice) pGABA neurons. (B_3 and D_3) Mean firing frequency before and during 10 s 3 μM farnesol application (mean ± SEM) for saline-treated pDA neurons (n = 4 neurons total from 3 mice) and saline-treated pGABA neurons (n = 4 neurons from 4 mice). In $B_{1\text{-}3}$ and $D_{1\text{-}3}$, lines indicate the individual neurons pre- and during nicotine puff. *, $p < 0.05$; **, $p < 0.01$; unpaired *t*-test. Exact *p* values are given in the *Results* section (***3.5***).

transiently transfected with α4-GFPβ2 or α6-GFPβ2β3 nAChRs with no-drug or 0.5 μM farnesol for 24 h. Following drug treatment we stimulated nAChRs with 10 μM nicotine. In α4-GFPβ2 nAChRs, we observed a non-significant ($p = 0.2$), 37% increase in peak current amplitude following farnesol treatment (Fig. 9$B_{1\text{-}2}$). In α6-GFPβ2β3 nAChRs we observed a 226%, increase ($p = 0.027$) in peak current amplitude following farnesol treatment (Fig. 9$D_{1\text{-}2}$).

4. Discussion

In this study, our aim was to determine if a chemical component of green apple flavor, farnesol, exhibits any evidence that it alters smoking-related behavior. While much attention has been placed on youth ENDS use, adults also heavily prefer flavored e-liquid products (70% of adults use flavored e-liquids compared to 90% of youth (Huang et al., 2019; Mead et al., 2019; Schneller et al., 2018). Therefore, it is critical that we understand how flavors in e-liquids alter smoking-related behaviors in both youth and adult populations. We chose farnesol for this study because of its structural similarity to menthol and it is the most prominent natural chemical flavorant of apples along with farnesene (Espino-Diaz et al., 2016) and is included in flavored cigarettes (prior to the 2009 ban), ENDS e-liquids (Aszyk et al., 2018), along with non-tobacco candies, perfumes, and beverages. Other flavorants for apple exist and are used in ENDS e-liquids such as hexyl acetate, ethyl acetate, and methylbutyl acetate (Tierney et al., 2016). Our observations of farnesol's actions support the need to study these other flavorants for their effect on reward-related behavior as well.

Here we document for the first time that a tobacco flavorant other than menthol alters reward-related behavior. The fact that farnesol by itself produced reward-related behavior is particularly relevant given the popularity of green apple flavor and the growing use of flavored, zero-nicotine e-liquids among ENDS users. From our observations, the observed farnesol-induced reward is at least in part caused by several changes in midbrain DA and GABA neurons (summarized in Fig. 10). On VTA DA neurons, α6* and α4α6* nAChRs are upregulated. This is accompanied by an increase in firing frequency of these VTA dopamine

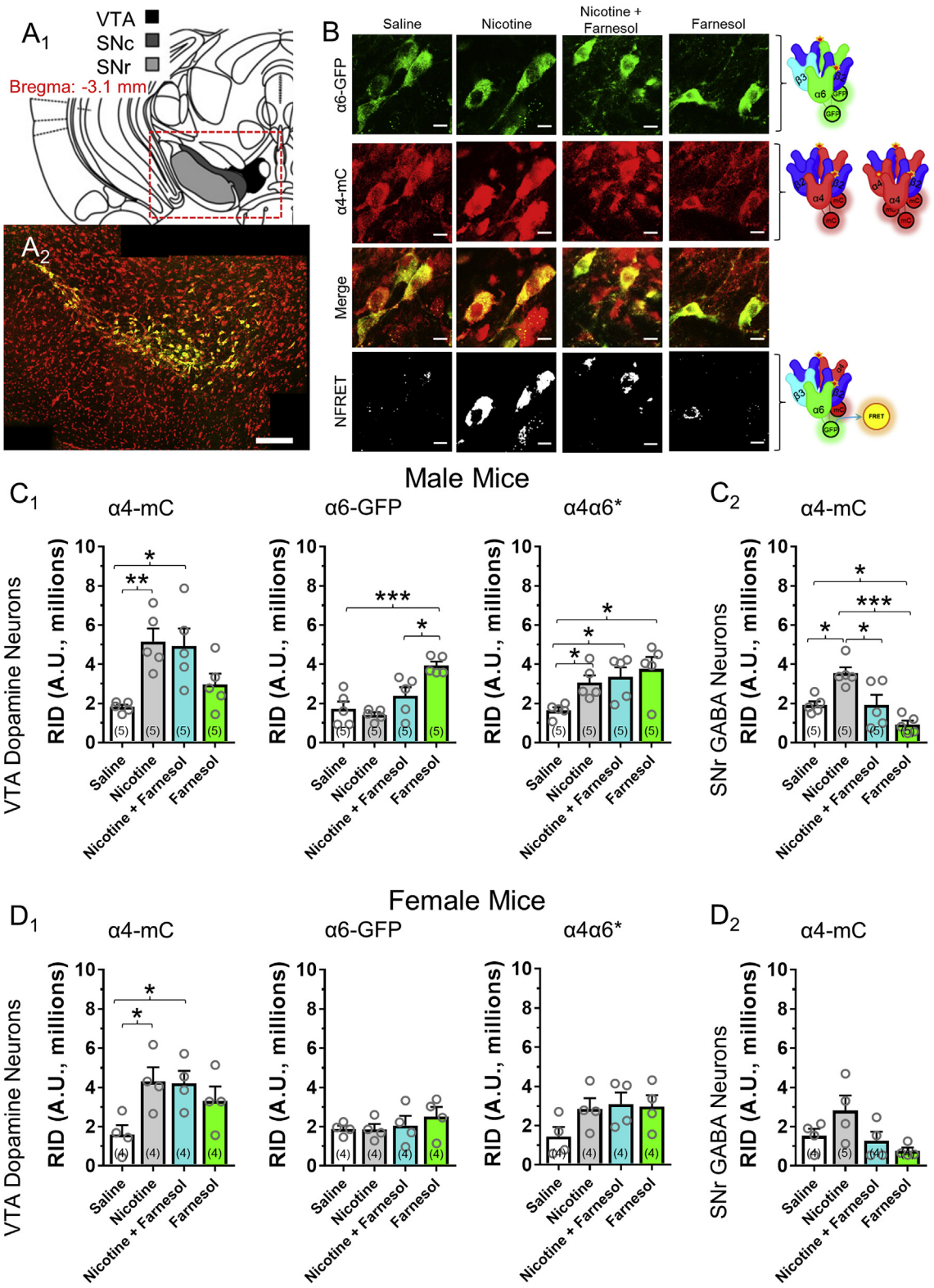

Fig. 8. Farnesol upregulates α6* and α4α6* nAChRs in VTA pDA neurons. (A_1) Schematic of our target mouse brain region in a coronal brain slice at bregma −3.1 mm (A_2) Montage of 10X images (scale bar, 100 μm) from a saline-treated α4-mCherryα6-GFP mouse at bregma −3.1 mm. (B) Representative images of neurons in the VTA following saline, nicotine, nicotine plus farnesol, or farnesol-alone treatment (from CPP assays). Scale bar, 10 μm. ($C_{1\text{-}2}$ and $D_{1\text{-}2}$) Raw integrated density (RID) of α4*, α6*, and α4α6* nAChRs on VTA pDA neurons or RID of α4* nAChRs in SNr GABA neurons in male ($C_{1\text{-}2}$) or female mice ($D_{1\text{-}2}$) from saline, nicotine, nicotine plus farnesol, or farnesol-alone treatment groups. Number in parenthesis indicates the number of mice used for each treatment group. Dots within bars indicate RID values from individual mice (n = 5 and 4 for male and female mice, respectively). *, $p < 0.05$; **, $p < 0.01$; ***, $p < 0.005$; one-way ANOVA with *post hoc* Bonferroni. Exact *p* values are given in the *Results* section (***3.6***).

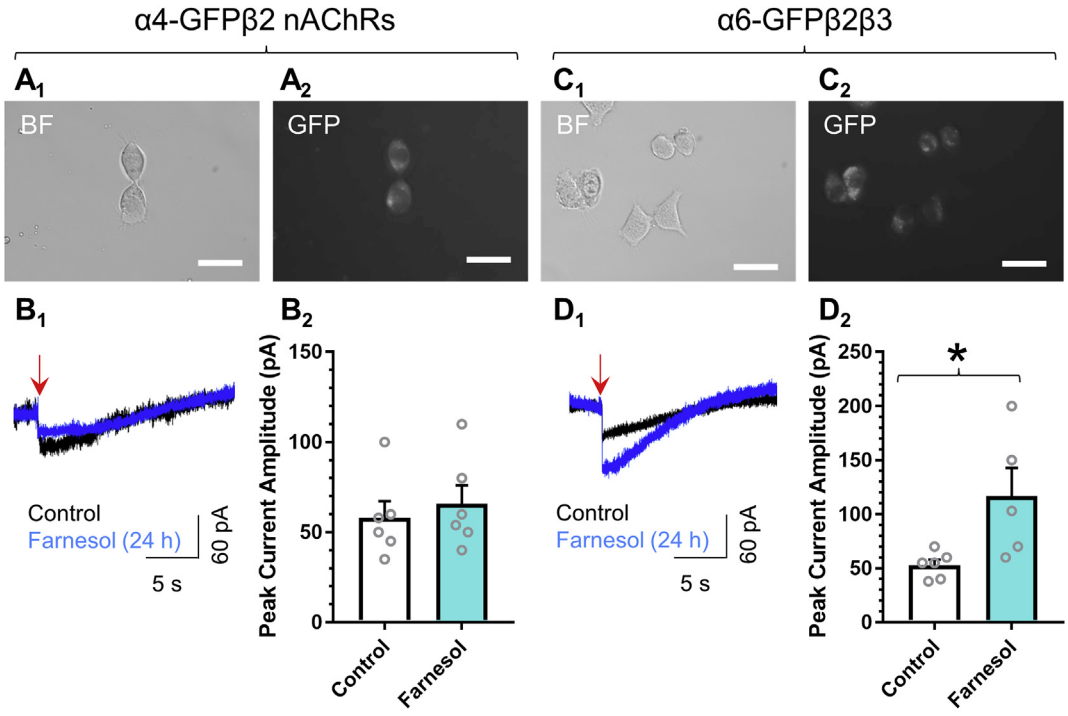

Fig. 9. Long-term farnesol treatment upregulates functional α6β2β3 nAChRs in neuro-2a cells. ($A_{1\text{-}2}$ and $C_{1\text{-}2}$) Representative neuro-2a cells transiently transfected with α4-GFPβ2 or α6-GFPβ2β3 nAChRs imaged in brightfield or GFP modes. Scale bars, 25 μm (B_1, D_1) Representative waveforms for control-treated (black) and farnesol-treated (blue) α4-GFPβ2 nAChRs (B_1) and α6-GFPβ2β3 nAChRs (D_1). (B_2 and D_2) Mean peak current amplitude of 300 ms puffs of 10 μM nicotine. Arrows indicate start of 300 ms puff. Data are mean ± SEM and individual dots represent individual cells (n = 5–6 cells, each condition). Exact *p* values are given in the Results section (***3.7***). (For interpretation of the references to colour in this figure legend, the reader is referred to the Web version of this article.)

neurons. Given that α6* and α4α6* nAChRs are high-affinity nAChRs that modulate excitability (Liu et al., 2012; Engle et al., 2013), their upregulation may be a significant factor in elevating the firing rate of VTA dopamine neurons. We must also consider the changes we observed in GABA neuron firing as well. Prior research into nicotine-induced changes in midbrain dopamine neuron firing revealed that much of this effect is a consequence of changes in GABA neuron firing (Nashmi et al., 2007; Xiao et al., 2009; Mansvelder et al., 2002). Given that we noted a farnesol-induced decrease in GABA neuron firing, we suggest that this also plays an important role in the observed farnesol-induced increase in DA neuron firing.

Since farnesol is a terpene that shares some chemical features with menthol, it is necessary to compare the effects of both flavors. Menthol combined with nicotine was previously characterized to enhance nicotine reward-related behavior; but menthol-alone, at several doses, failed to produce reward (Henderson et al., 2017), reinforcement (Wang et al., 2014), or elevation of dopamine release (Wickham et al., 2018). Unlike menthol, farnesol by itself was found to produce reward-related behavior. To answer the question of how farnesol can stimulate reward while menthol does not, we must consider their differing effects. In comparing menthol's and farnesol's effect on midbrain dopamine neurons: menthol-alone decreases VTA pDA neuron baseline firing frequency (Henderson et al., 2016) but farnesol-alone increases VTA pDA firing frequency. Furthermore, we note that following long-term menthol treatment, stimulating DA neurons resulted in a transient silencing of pDA neuron firing (Henderson et al., 2016). Here, we observed that after farnesol treatment, stimulating pDA or pGABA neurons with 500 nM nicotine still produces a transient increase in firing

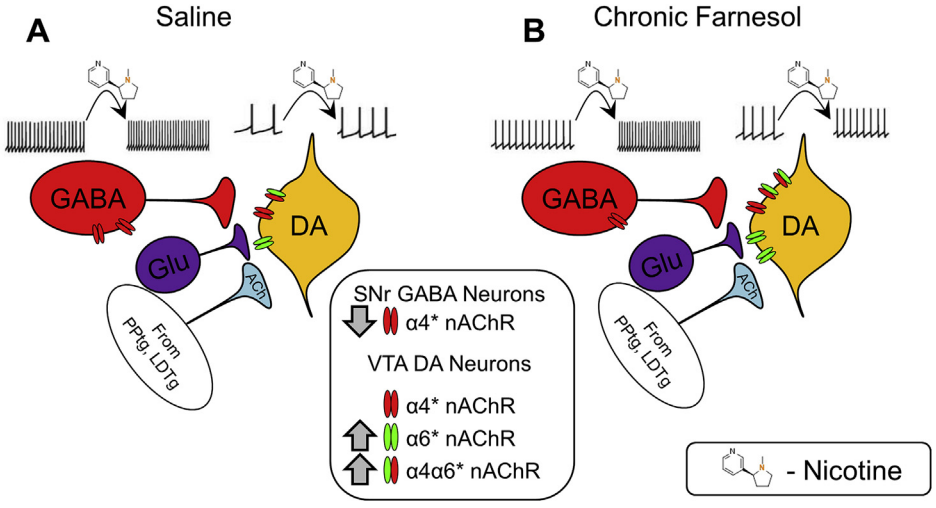

Fig. 10. Summary of farnesol's effect on midbrain neurons. VTA dopamine neurons receive excitatory inputs from local/distant glutamate (Glu) neurons and cholinergic neurons but inhibitory input from GABA neurons. Compared to saline-treated dopamine neurons (A), farnesol-treated neurons (B) exhibit an increase in α4α6* and α6* nAChRs and elevated action potential frequency. This elevation in dopamine neuron firing frequency is likely a consequence of decreased activity from inhibitory GABA neurons. PPtg, pedunculopontine tegmental nucleus; LDTg, laterodorsal tegmental nucleus.

frequency (Fig. 7). This difference suggests that treatment with menthol-alone significantly impairs pDA neuron excitability while farnesol treatment allows pDA neurons to remain excitable.

A second important observation is that at doses relevant for reward-related behavior assays (CPP) menthol only upregulates α4α6* nAChRs. Conversely, farnesol significantly upregulates α4α6* and α6* nAChRs (Figs. 8 and 9). While it is unclear how upregulation may play a direct role in reward-related behavior, it is clear that the presence of α4*, α6*, and α4α6* nAChRs are necessary for nicotine reward or reinforcement (Pons et al., 2008). It is possible that α6* nAChRs play a specific role in the initiation of nicotine reward (or reward-related behavior in general) and the increased number of α6* nAChRs may be an important component in the farnesol-induced reward we observed. This is supported by the observation that we only noted α6* upregulation in males and it was only male mice that exhibited reward to farnesol-alone. Conversely, females displayed no reward-related behavior to farnesol-alone and did not exhibit upregulation of α6* nAChRs. Despite this observation, more extensive studies are needed to increase our understanding of how α6* and α4α6* nAChRs contribute to different stages of nicotine reward or reinforcement.

Despite the sex-dependent effects of farnesol on reward-related behavior, pDA neuron firing frequency, and α6* nAChR upregulation we did not observe a sex-dependent effect on mouse locomotor behavior (see section 3.3). Many nicotinic ligands can modulate acute changes in locomotor behavior but these are typically agonists or partial agonists of nAChRs (Baker et al., 2013; Wall et al., 2017). However, it has been previously determined that mouse cholinergic modulation of locomotor activity has been tied to α6β2* and α4α6β2* nAChRs (Drenan et al., 2010; Cohen et al., 2012). Given our observations that farnesol exhibits a potentially selective effect on α6* and not α4* nAChRs, it is possible that α6β2* and α4α6β2* nAChRs are modulated by acute farnesol concentrations that are sufficient to modulate locomotor activity. While we did not note any effect with farnesol-treated female mice in physiology or microscopy assays, we note that the time-points for these assays are different than that of our acute locomotor assays. In our locomotor assays, our observational endpoint started immediately after injection of farnesol. For both electrophysiology and microscopy, our time-point was locked by our CPP paradigm and brains were extracted and studied ~24 h after the final injection. Additionally, to further investigate this connection to locomotor behavior our investigation would need to extend to the SNc, as these neurons project to the dorsal striatum and are chiefly responsible for the cholinergic and dopaminergic modulation of locomotor behavior in mice (Cohen et al., 2012).

5. Conclusions

It is becoming clear that flavored tobacco products increase smoking initiation and reduce cessation. For this reason, the FDA enacted a ban on flavored (excluding menthol) combustible cigarettes as part of the 2009 Family Smoking Prevention Act. Currently, a critical component of the FDA's Tobacco Prevention Plan is targeting potential restrictions on flavored e-liquids (www.fda.gov). Our data presented here suggest that tobacco flavors may increase the addictive potential of ENDS and may also explain why smokers prefer flavored products and flavored e-liquids (Schauer et al., 2018). We believe this data supports the investigation of other flavors and additional flavorants of green apple in regard to their role in addiction and smoking behavior.

Contributions

Behavioral assays were performed by ATA, GPC, SYC, and BJH. Electrophysiology was performed by BJH. Microscopy was performed by AJA, ATA, ZBJ, SYC, and BJH. Funding was secured by BJH. The paper was written by BJH and all authors participated in editing.

Funding and disclosure

Research reported in this publication was supported by National Institute on Drug Abuse (NIDA) and FDA Center for Tobacco Products (CTP) grant DA046335. The content is solely the responsibility of the authors and does not necessarily represent the official views of the NIH or the Food and Drug Administration. Funding was also provided by NIDA grant DA040047.

Appendix A. Supplementary data

Supplementary data to this article can be found online at https://doi.org/10.1016/j.neuropharm.2019.107729.

References

Alsharari, S.D., King, J.R., Nordman, J.C., Muldoon, P.P., Jackson, A., Zhu, A.Z.X., Tyndale, R.F., Kabbani, N., Damaj, M.I., 2015. Effects of menthol on nicotine pharmacokinetic, pharmacology and dependence in mice. PLoS One 10, e0137070.

Antoniou, K., Papathanasiou, G., Papalexi, E., Hyphantis, T., Nomikos, G.G., Spyraki, C., Papadopoulou-Daifoti, Z., 2008. Individual responses to novelty are associated with differences in behavioral and neurochemical profiles. Behav. Brain Res. 187, 462–472.

Aszyk, J., Kubica, P., Wozniak, M.K., Namiesnik, J., Wasik, A., Kot-Wasik, A., 2018. Evaluation of flavour profiles in e-cigarette refill solutions using gas chromatography-tandem mass spectrometry. J. Chromatogr. A 1547, 86–98.

Baker, L.K., Mao, D., Chi, H., Govind, A.P., Vallejo, Y.F., Iacoviello, M., Herrera, S., Cortright, J.J., Green, W.N., McGehee, D.S., Vezina, P., 2013. Intermittent nicotine exposure upregulates nAChRs in VTA dopamine neurons and sensitises locomotor responding to the drug. Eur. J. Neurosci. 37, 1004–1011.

Benowitz, N.L., Samet, J.M., 2011. The threat of menthol cigarettes to U.S. public health. N. Engl. J. Med. 364, 2179–2181.

Biswas, L., Harrison, E., Gong, Y., Avusula, R., Lee, J., Zhang, M., Rousselle, T., Lage, J., Liu, X., 2016. Enhancing effect of menthol on nicotine self-administration in rats. Psychopharmacology (Berlin) 233, 3417–3427.

Brody, A., Mukhin, A., La Charite, J., Ta, K., Farahi, J., Sugar, C., Mamoun, M., Vellios, E., Archie, M., Kozman, M., Phuong, J., Arlorio, F., Mandelkern, M., 2013. Up-regulation of nicotinic acetylcholine receptors in menthol cigarette smokers. Int. J. Neuropsychopharmacol. 16, 957–966.

Cohen, B.N., Mackey, E.D., Grady, S.R., McKinney, S., Patzlaff, N.E., Wageman, C.R., McIntosh, J.M., Marks, M.J., Lester, H.A., Drenan, R.M., 2012. Nicotinic cholinergic mechanisms causing elevated dopamine release and abnormal locomotor behavior. Neuroscience 200, 31–41.

D'Silva, J., Boyle, R.G., Lien, R., Rode, P., Okuyemi, K.S., 2012. Cessation outcomes among treatment-seeking menthol and nonmenthol smokers. Am. J. Prev. Med. 43, S242–S248.

Delnevo, C.D., Gundersen, D.A., Hrywna, M., Echeverria, S.E., Steinberg, M.B., 2011. Smoking-cessation prevalence among U.S. smokers of menthol versus non-menthol cigarettes. Am. J. Prev. Med. 41, 357–365.

Deng, P., Zhang, Y., Xu, Z.C., 2007. Involvement of I(h) in dopamine modulation of tonic firing in striatal cholinergic interneurons. J. Neurosci. 27, 3148–3156.

Dessirier, J.M., O'Mahony, M., Carstens, E., 2001. Oral irritant properties of menthol: sensitizing and desensitizing effects of repeated application and cross-desensitization to nicotine. Physiol. Behav. 73, 25–36.

Drenan, R.M., Nashmi, R., Imoukhuede, P.I., Just, H., McKinney, S., Lester, H.A., 2008. Subcellular trafficking, pentameric assembly and subunit stoichiometry of neuronal nicotinic ACh receptors containing fluorescently-labeled α6 and β3 subunits. Mol. Pharmacol. 73, 27–41.

Drenan, R.M., Grady, S.R., Steele, A.D., McKinney, S., Patzlaff, N.E., McIntosh, J.M., Marks, M.J., Miwa, J.M., Lester, H.A., 2010. Cholinergic modulation of locomotion and striatal dopamine release is mediated by α6α4* nicotinic acetylcholine receptors. J. Neurosci. 30, 9877–9889.

Engle, S.E., Shih, P.Y., McIntosh, J.M., Drenan, R.M., 2013. α4α6β2* nicotinic acetylcholine receptor activation on ventral tegmental area dopamine neurons is sufficient to stimulate a depolarizing conductance and enhance surface AMPA receptor function. Mol. Pharmacol. 84, 393–406.

Espino-Diaz, M., Sepulveda, D.R., Gonzalez-Aguilar, G., Olivas, G.I., 2016. Biochemistry of apple aroma: a review. Food Technol. Biotechnol. 54, 375–397.

Fan, L., Balakrishna, S., Jabba, S.V., Bonner, P.E., Taylor, S.R., Picciotto, M.R., Jordt, S.-E., 2016. Menthol decreases oral nicotine aversion in C57BL/6 mice through a TRPM8-dependent mechanism. Tob. Control 0, 1–5.

FDA, 2012. Preliminary Scientific Evaluation of the Possible Public Health Effects of Menthol versus Nonmenthol Cigarettes. https://www.fda.gov/downloads/ucm361598.pdf.

Gandhi, K.K., Foulds, J., Steinberg, M.B., Lu, S.E., Williams, J.M., 2009. Lower quit rates among African American and Latino menthol cigarette smokers at a tobacco treatment clinic. Int. J. Clin. Pract. 63, 360–367.

Hans, M., Wilhelm, M., Swandulla, D., 2012. Menthol suppresses nicotinic acetylcholine receptor functioning in sensory neurons via allosteric modulation. Chem. Senses 37, 463–469.

Henderson, B.J., Lester, H.A., 2015. Inside-out neuropharmacology of nicotinic drugs.

Neuropharmacology 96 (Pt. B), 178–193.
Henderson, B.J., Wall, T.R., Henley, B.M., Kim, C.H., McKinney, S., Lester, H.A., 2017. Menthol enhances nicotine reward-related behavior by potentiating nicotine-induced changes in nAChR function, nAChR upregulation, and DA neuron excitability. Neuropsychopharmacology. https://doi.org/10.1038/npp.2017.72.
Henderson, B.J., Wall, T., Henley, B.M., Kim, C.H., Nichols, W.A., Moaddel, R., Xiao, C., Lester, H.A., 2016. Menthol alone upregulates midbrain nAChRs, alters nAChR subtype stoichiometry, alters dopamine neuron firing frequency, and prevents nicotine reward. J. Neurosci. 36.
Henderson, B.J., Srinivasan, R., Nichols, W.A., Dilworth, C.N., Gutierrez, D.F., Mackey, E.D., McKinney, S., Drenan, R.M., Richards, C.I., Lester, H.A., 2014. Nicotine exploits a COPI-mediated process for chaperone-mediated up-regulation of its receptors. J. Gen. Physiol. 143, 51–66.
Hoffman, A.C., Miceli, D., 2011. Menthol cigarettes and smoking cessation behavior. Tob. Induc. Dis. 9 (Suppl. 1), S6.
Huang, J., Duan, Z., Kwok, J., Binns, S., Vera, L.E., Kim, Y., Szczypka, G., Emery, S.L., 2019. Vaping versus JUULing: how the extraordinary growth and marketing of JUUL transformed the US retail e-cigarette market. Tob. Control 28 (2), 146–151. https://doi.org/10.1136/tobaccocontrol-2018-054382.
Jasinska, A.J., Zorick, T., Brody, A.L., Stein, E.A., 2014. Dual role of nicotine in addiction and cognition: a review of neuroimaging studies in humans. Neuropharmacology 84, 111–122. https://doi.org/10.1016/j.neuropharm.2013.02.015.
Kuryatov, A., Lindstrom, J., 2011. Expression of functional human α6β2β3 acetylcholine receptors in *Xenopus* laevis oocytes achieved through subunit chimeras and concatamers. Mol. Pharmacol. 79, 126–140.
Liu, L., Zhao-Shea, R., McIntosh, J.M., Gardner, P.D., Tapper, A.R., 2012. Nicotine persistently activates ventral tegmental area dopaminergic neurons via nicotinic acetylcholine receptors containing α4 and α6 subunits. Mol. Pharmacol. 81, 541–548.
Lynch III, J.J., Mittelstadt, S.W., 2009. Can locomotor screening be utilized as a first-tiered approach for pre-clinical CNS/neurobehavioral safety testing? J. Pharmacol. Toxicol. Methods 60, 232.
Mackey, E.D., Engle, S.E., Kim, M.R., O'Neill, H.C., Wageman, C.R., Patzlaff, N.E., Wang, Y., Grady, S.R., McIntosh, J.M., Marks, M.J., Lester, H.A., Drenan, R.M., 2012. α6* nicotinic acetylcholine receptor expression and function in a visual salience circuit. J. Neurosci. 32, 10226–10237.
Mansvelder, H.D., Keath, J.R., McGehee, D.S., 2002. Synaptic mechanisms underlie nicotine-induced excitability of brain reward areas. Neuron 33, 905–919.
Mead, E.L., Duffy, V., Oncken, C., Litt, M.D., 2019. E-cigarette palatability in smokers as a function of flavorings, nicotine content and propylthiouracil (PROP) taster phenotype. Addict. Behav. 91, 37–44. https://doi.org/10.1016/j.addbeh.2018.11.014.
Mukhin, A.G., Kimes, A.S., Chefer, S.I., Matochik, J.A., Contoreggi, C.S., Horti, A.G., Vaupel, D.B., Pavlova, O., Stein, E.A., 2008. Greater nicotinic acetylcholine receptor density in smokers than in nonsmokers: a PET study with 2-18F-FA-85380. J. Nucl. Med. 49, 1628–1635.
Nashmi, R., Dickinson, M.E., McKinney, S., Jareb, M., Labarca, C., Fraser, S.E., Lester, H.A., 2003. Assembly of α4β2 nicotinic acetylcholine receptors assessed with functional fluorescently labeled subunits: effects of localization, trafficking, and nicotine-induced upregulation in clonal mammalian cells and in cultured midbrain neurons. J. Neurosci. 23, 11554–11567.
Nashmi, R., Xiao, C., Deshpande, P., McKinney, S., Grady, S.R., Whiteaker, P., Huang, Q., McClure-Begley, T., Lindstrom, J.M., Labarca, C., Collins, A.C., Marks, M.J., Lester, H.A., 2007. Chronic nicotine cell specifically upregulates functional α4* nicotinic receptors: basis for both tolerance in midbrain and enhanced long-term potentiation in perforant path. J. Neurosci. 27, 8202–8218.
Omaiye, E.E., McWhirter, K.J., Luo, W., Tierney, P.A., Pankow, J.F., Talbot, P., 2019. High concentrations of flavor chemicals are present in electronic cigarette refill fluids. Sci. Rep. 9, 2468.
Perez, X.A., Bordia, T., McIntosh, J.M., Grady, S.R., Quik, M., 2008. Long-term nicotine treatment differentially regulates striatal α6α4β2* and α6(Nonα4)β2* nAChR expression and function. Mol. Pharmacol. 74, 844–853.
Pons, S., Fattore, L., Cossu, G., Tolu, S., Porcu, E., McIntosh, J.M., Changeux, J.P., Maskos, U., Fratta, W., 2008. Crucial role of α4 and α6 nicotinic acetylcholine receptor subunits from ventral tegmental area in systemic nicotine self-administration. J. Neurosci. 28, 12318–12327.
Sallette, J., Pons, S., Devillers-Thiery, A., Soudant, M., Prado de Carvalho, L., Changeux, J.P., Corringer, P.J., 2005. Nicotine upregulates its own receptors through enhanced intracellular maturation. Neuron 46, 595–607.
Sanjakdar, S.S., Maldoon, P.P., Marks, M.J., Brunzell, D.H., Maskos, U., McIntosh, J.M., Bowers, M.S., Damaj, M.I., 2015. Differential roles of α6β2* and α4β2* neuronal nicotinic receptors in nicotine- and cocaine-conditioned reward in mice. Neuropsychopharmacology 40, 350–360.
Schauer, G.L., Peters, E.N., Rosenberry, Z.R., Kim, H., 2018. Trends in and characteristics of Marijuana and menthol cigarette use among current cigarette smokers, 2005-2014. Nicotine Tob. Res. 20, 362–369.
Schneller, L.M., Bansal-Travers, M., Goniewicz, M.L., McIntosh, S., Ossip, D., O'Connor, R.J., 2018. Use of flavored electronic cigarette refill liquids among adults and youth in the US-Results from Wave 2 of the Population Assessment of Tobacco and Health Study (2014-2015). PLoS One 13, e0202744.
Srinivasan, R., Pantoja, R., Moss, F.J., Mackey, E.D.W., Son, C., Miwa, J., Lester, H.A., 2011. Nicotine upregulates α4β2 nicotinic receptors and ER exit sites via stoichiometry-dependent chaperoning. J. Gen. Physiol. 137, 59–79.
Srinivasan, R., Henley, B.M., Henderson, B.J., Indersmitten, T., Cohen, B.N., Kim, C.H., McKinney, s, Deshpande, P., Xiao, C., Lester, H.A., 2016. Smoking-relevant nicotine concentration attenuates the unfolded protein response in dopaminergic neurons. J. Neurosci. 36, 65–79.
Tapper, A.R., McKinney, S.L., Nashmi, R., Schwarz, J., Deshpande, P., Labarca, C., Whiteaker, P., Marks, M.J., Collins, A.C., Lester, H.A., 2004. Nicotine activation of α4* receptors: sufficient for reward, tolerance and sensitization. Science 306, 1029–1032.
Tierney, P.A., Karpinski, C.D., Brown, J.E., Luo, W., Pankow, J.F., 2016. Flavour chemicals in electronic cigarette fluids. Tob. Control 25, e10–15.
Wall, T.R., Henderson, B.J., Voren, G., Wageman, C.R., Deshpande, P., Cohen, B.N., Grady, S.R., Marks, M.J., Yohannes, D., Bencherif, M., Kenny, P.J., Lester, H.A., 2017. TC299423, a novel agonist for nicotinic acetylcholine receptors. Front. Pharmacol 8, 641. https://doi.org/10.3389/fphar.2017.00641.
Wang, T., Wang, B., Chen, H., 2014. Menthol facilitates the intravenous self-administration of nicotine in rats. Front. Behav. Neurosci. 8, 437.
Wickham, R.J., Nunes, E.J., Hughley, S., Silva, P., Walton, S.N., Park, J., Addy, N.A., 2018. Evaluating oral flavorant effects on nicotine self-administration behavior and phasic dopamine signaling. Neuropharmacology 128, 33–42.
Xiao, C., Nashmi, R., McKinney, S., Cai, H., McIntosh, J.M., Lester, H.A., 2009. Chronic nicotine selectively enhances α4β2* nicotinic acetylcholine receptors in the nigrostriatal dopamine pathway. J. Neurosci. 29, 12428–12439.
Xiao, C., Srinivasan, R., Drenan, R.M., Mackey, E.D., McIntosh, J.M., Lester, H.A., 2011. Characterizing functional α6β2 nicotinic acetylcholine receptors in vitro: mutant β2 subunits improve membrane expression, and fluorescent proteins reveal responsive cells. Biochem. Pharmacol. 82, 852–861.
Xiao, C., Miwa, J.M., Henderson, B.J., Wang, Y., Deshpande, P., McKinney, S.L., Lester, H.A., 2015. Nicotinic receptor subtype-selective circuit patterns in the subthalamic nucleus. J. Neurosci. 35, 3734–3746.
Zhang, M., Harrison, E., Biswas, L., Tran, T., Liu, X., 2018. Menthol facilitates dopamine-releasing effect of nicotine in rat nucleus accumbens. Pharmacol. Biochem. Behav. 175, 47–52.